

Non-local slicing approaches for NNLO QCD in MCFM

John M. Campbell,^a R. Keith Ellis,^b Satyajit Seth^c

^a*Fermilab, PO Box 500, Batavia IL 60510-5011, USA*

^b*Institute for Particle Physics Phenomenology, Durham University, Durham, DH1 3LE, UK*

^c*Physical Research Laboratory, Navrangpura, Ahmedabad - 380009, India*

E-mail: johnmc@fnal.gov, keith.ellis@durham.ac.uk, seth@prl.res.in

ABSTRACT: We present the implementation of several processes at Next-to-Next-to Leading Order (NNLO) accuracy in QCD in the parton-level Monte Carlo program MCFM. The processes treated are $pp \rightarrow H, W^\pm, Z, W^\pm H, ZH, W^\pm \gamma, Z\gamma$ and $\gamma\gamma$ and, for the first time in the code, W^+W^- , $W^\pm Z$ and ZZ . Decays of the unstable bosons are fully included, resulting in a flexible fully differential Monte Carlo code. The NNLO corrections have been calculated using two non-local slicing approaches, isolating the doubly unresolved region by cutting on the zero-jettiness, \mathcal{T}_0 , or on q_T , the transverse momentum of the colour singlet final-state particles. We find that for most, but not all processes the q_T slicing method leads to smaller power corrections for equal computational burden.

KEYWORDS: QCD, Helicity Amplitudes, Vector bosons

Contents

1	Introduction	1
2	Non-local slicing methods	3
2.1	Non-local jettiness slicing	4
2.2	Non-local q_T slicing	5
2.3	Hard functions	6
2.4	Above cut contributions	6
3	Comparative study of jettiness and q_T slicing	6
3.1	Processes and cuts	8
3.2	Input parameters	8
3.3	NLO	9
3.4	NNLO	15
3.5	Comparison with Ref. [1]	17
4	Conclusion	22
A	Leading log behaviour of colour singlet production cross section	23
B	Translation of two-loop corrections to the hard function	24
C	Cuts	25

1 Introduction

The current and future success of the LHC depends crucially on the precision supplied by theoretical calculations. Reducing the theoretical error has special importance in the context of Higgs Physics[2] where for many channels it is projected to remain the largest error at the conclusion of the LHC program.

An important role is played by processes involving the bosons, W, Z, γ and H . The importance of detailed studies of the Higgs boson goes without saying. Single vector boson production can be used as a luminosity monitor and to probe parton distribution functions. Electroweak production of vector boson pairs is a stringent test of the standard model. In addition the $\gamma\gamma$, ZZ , WW and $Z\gamma$ processes have renewed significance because they constitute backgrounds to Higgs boson decay processes.

We are preparing a release of MCFM [3–6] which will allow calculation of the NNLO QCD results for a large number of colour singlet production processes with both zero-jettiness [7–9] and q_T -slicing [10].¹ The code has also been used for processes with non-colour singlet final states, such as $W + \text{jet}$ [8], $Z + \text{jet}$ [11], $\gamma + \text{jet}$ [12], and Higgs boson +

¹We aim to release this version in March 2022.

jet [13, 14], although these have not yet been made available in the public version. These latter processes are treatable because of the SCET factorization theorems for the cross sections for small 1-jettiness.

Given the importance of precision for the LHC, there has been an intense community effort to produce results at NNLO QCD and in some cases N³LO. A review of the 2020 status of precision QCD with a special focus on the Higgs boson is given in Ref. [15]. In Table 1 we present references for the processes that have been calculated in NNLO QCD. It is important to note that when targeting the precision achievable at NNLO, electroweak corrections can also become important, especially at large p_T . A discussion of these effects is beyond the scope of this paper.

In Ref. [21] MCFM results for $pp \rightarrow H$, $pp \rightarrow Z$, $pp \rightarrow W$, $pp \rightarrow ZH$, $pp \rightarrow WH$ and $pp \rightarrow \gamma\gamma$ have been presented. Results for colour singlet production processes, especially vector boson pairs have also been presented by the MATRIX collaboration [24, 88]. Therefore, although results for the colour singlet cross sections presented in this paper are known, in view of the complicated nature of these calculations it is re-assuring to have an independent check. The results of Ref. [24, 88] calculate one-loop virtual corrections using Openloops 2 [89], whereas in MCFM the one-loop virtual corrections are calculated analytically, with consequent benefits for the stability and speed of this portion of the code. Note however that the MATRIX and MCFM calculations for vector boson pairs can not be

Process	MCFM	Process	MCFM
$H + 0 \text{ jet}$ [9, 10, 16–20]	✓ [21]	$W^\pm + 0 \text{ jet}$ [22–24]	✓ [21]
$Z/\gamma^* + 0 \text{ jet}$ [9, 23–25]	✓ [21]	ZH [26]	✓ [27]
$W^\pm \gamma$ [24, 28, 29]	✓ [30]	$Z\gamma$ [24, 31]	✓ [31]
$\gamma\gamma$ [24, 32–34]	✓ [35]	single top [36]	✓ [37]
$W^\pm H$ [38, 39]	✓ [27]	WZ [40, 41]	✓
ZZ [1, 24, 42–46]	✓	W^+W^- [24, 47–50]	✓
$W^\pm + 1 \text{ jet}$ [51, 52]	[8]	$Z + 1 \text{ jet}$ [53, 54]	[11]
$\gamma + 1 \text{ jet}$ [55]	[12]	$H + 1 \text{ jet}$ [56–61]	[13]
$b\bar{b} \rightarrow H + \text{jet}$	[14]		
$t\bar{t}$ [62–67]		$Z + b$ [68]	
$W^\pm H + \text{jet}$ [69]		$ZH + \text{jet}$ [70]	
Higgs WBF [71, 72]		$H \rightarrow b\bar{b}$ [73–75]	
top decay [37, 76, 77]		dijets [78–80]	
$\gamma\gamma + \text{jet}$ [81]		$W^\pm c$ [82]	
$b\bar{b}$ [83]		$\gamma\gamma\gamma$ [84, 85]	
HH [86]		HHH [87]	

Table 1. Publications on processes evaluated differentially at NNLO, (and in some cases beyond NNLO). The tick mark indicates that the process is available in the public MCFM version. Processes with a reference but no tickmark are not yet in the public MCFM code. Processes with a tickmark but no reference have been introduced into the public code at this time.

considered totally independent, relying as they do on the same two-loop amplitudes [90, 91]. We also compare with an calculation of ZZ production [1], which is independent (except for the same caveat about two-loop matrix elements).

Recently there has been a detailed re-examination of fiducial cross sections for two-body decay processes at colliders, demonstrating that certain commonly used cuts are sensitive to low momentum scales [92, 93].² Where possible we shall limit our discussion in this paper to total inclusive cross sections, leaving detailed predictions with well-motivated cuts to a subsequent paper.

A successive improvement of our results could come from widespread inclusion of resummation effects along the lines of Refs. [96, 97]. Resummation effects in vector boson pair production have previously been considered in Refs. [98–100]. Resummation is also part of the program in the GENEVA collaboration. Ref. [101] provides a recent article, where references to earlier work of the GENEVA collaboration can be found.

2 Non-local slicing methods

In this section we review the calculation of the NNLO cross sections which have colour singlet final states at the Born level. The necessary requisites for the methods are,

- An analytic understanding of the behaviour of the Born process accompanied by soft and collinear radiation through to the requisite order, i.e. for NNLO through to order α_s^2 .
- A NLO calculation of the process at hand with one additional parton.
- The two-loop virtual corrections to the process at hand, necessary to calculate the hard function at order α_s^2

Let r be a zero jet resolution variable which divides the phase space in two,

$$\sigma(X) = \sigma(X, r^{cut}) + \int_{r^{cut}} dr' \frac{d\sigma(X)}{dr'}, \quad (2.1)$$

where X represents other kinematics on the phase space. In the following subsections we shall take the resolution variable, r^{cut} to be either the 0-jettiness, \mathcal{T}_0 or the transverse momentum, q_T of the final state.

$$\sigma(X, r^{cut}) = \int^{r^{cut}} dr' \frac{d\sigma(X)}{dr'}. \quad (2.2)$$

The cross section is given by introducing σ^{sub} , the analytic form for the cross section, known for small values of the resolution parameter r^{cut} from factorization theorems.

$$\sigma = \sigma^{sub}(r^{cut}) + \int^{r^{cut}} dr' \frac{d\sigma(X)}{dr'} + [\sigma(r^{cut}) - \sigma^{sub}(r^{cut})]$$

²Methods to remove the dominant (linear) sensitivity in the low-momentum region in a fully differential way, for the q_T -slicing method, have been developed in Refs. [94, 95].

$$\equiv \sigma^{sub}(r^{cut}) + \int^{r^{cut}} dr' \frac{d\sigma(X)}{dr'} + [\Delta\sigma(r^{cut})]. \quad (2.3)$$

Since r is a zero jet resolution variable, $\Delta\sigma(r^{cut})$ will tend to zero as $r^{cut} \rightarrow 0$.

2.1 Non-local jettiness slicing

The 0-jettiness slicing method is based on the corresponding event shape introduced in Ref. [7]. Writing q^μ, Q and Y for the four-momentum, mass and rapidity of the colour singlet system in its centre of mass, the incoming parton momenta are

$$p_i = x_i E_{cm} \frac{n}{2}, \quad p_j = x_j E_{cm} \frac{\bar{n}}{2}, \quad (2.4)$$

where $n = (1, +\vec{z})$, $\bar{n} = (1, -\vec{z})$. The zero-jettiness in the colour singlet centre of mass is then defined by,

$$\mathcal{T}_0 = \sum_k \min\{e^{+Y} p_k^+, e^{-Y} p_k^-\}, \quad (2.5)$$

where the sum over k runs over all final state partons and $p_k^- = p \cdot n$, $p_k^+ = p \cdot \bar{n}$. The all-orders resummed form of the cross section in the region of small \mathcal{T}_0 , obtained by application of soft-collinear effective theory (SCET) [102–106], is then given by,

$$\frac{d\sigma}{d\mathcal{T}_0} = \sum_{ij} \int dx_i dx_j \int d\Phi_B(p_i, p_j; p_{\text{singlet}}) H_{ij}(\Phi_B, \mu) \frac{d\Delta_{ij}}{d\mathcal{T}_0} + \dots, \quad (2.6)$$

where the indices i, j run over all initial state partons involved in the scattering. Φ_B represents the Born-level color singlet phase space $p_i p_j \rightarrow p_{\text{singlet}}$ and H_{ij} the hard function. The soft/collinear function Δ_{ij} is,

$$\begin{aligned} \frac{d\Delta_{ij}}{d\mathcal{T}_0} &= B_{i/H_1} \otimes B_{j/H_2} \otimes S_{ij} \\ &\equiv \int dt_{B_i} dt_{B_j} dt_S \delta(\mathcal{T}_0 - t_{B_i} - t_{B_j} - t_S) B_{i/H_1}(t_{B_i}, x_i) B_{j/H_2}(t_{B_j}, x_j) S_{ij}(t_S) \end{aligned} \quad (2.7)$$

The hard function encodes both the leading order matrix elements and perturbative virtual corrections as described later in section 2.3. The beam function $B_{i/H}$ describes initial-state collinear radiation from hadron H and can be written as a convolution of perturbative matching coefficients and the usual parton density functions, $f_{i/H}$. It has been computed up to two loops in Refs. [107, 108]. The effects of soft radiation are collected in the soft function S , which has been calculated for zero-jettiness up to two-loop order in Refs. [109, 110].

In the color singlet centre of mass frame the power corrections to the factorization in Eq. (2.6) are known to be reduced [111]. Power corrections to the simplest $2 \rightarrow 1$ processes are known [111–115] but, since they are not known universally and we also wish to compare with the q_T approach, we do not include them in this study.

2.2 Non-local q_T slicing

In this section we briefly describe the calculation using the transverse momentum as a resolution parameter. Although the formalism we describe is not the formalism in which q_T slicing was originally implemented [116–121] it is simplest to implement q_T slicing using the factorized form of the low q_T cross section derived using SCET. Schematically, the differential cross section takes the form,

$$\frac{d^2\sigma}{dQ dq_T} \sim \tilde{\mathcal{B}}_{i/H_1}(x_1, k_{1T}, \mu; \xi_1) \otimes \tilde{\mathcal{B}}_{j/H_2}(x_2, k_{2T}, \mu; \xi_2) \otimes \tilde{\mathcal{S}}_{ij}(q_T, \mu; \xi_1, \xi_2) \otimes H_{ij}(z, Q, \mu), \quad (2.8)$$

where the symbol \otimes denotes a convolution. Note that the soft function $\tilde{\mathcal{S}}$ and the naive transverse PDFs $\tilde{\mathcal{B}}$ depend on unphysical parameters, ξ_1 and ξ_2 . However, in physical cross sections the dependence on these parameters appears in such a way that only the physical scale Q remains.

The $\tilde{\mathcal{B}}$ and $\tilde{\mathcal{S}}$ functions still depend on both Q and q_T , two disparate scales. As such, Eq. (2.8) does not represent a true factorization and thus additional work must be performed to isolate the dependence on the scale Q . We follow the SCET re-factorization approach of [122, 123]. Thus for the simplest Drell-Yan process we have,

$$\begin{aligned} \frac{d^3\sigma}{dQ^2 dq_T^2 dy} &= \frac{\alpha^2}{3N_c Q^2 s} \sum_{i,j} \sum_q e_q^2 [C_{q\bar{q} \leftarrow ij}(z_1, z_2, q_T^2, Q^2, \mu) + (q \leftrightarrow \bar{q})] \\ &\quad \otimes f_{i/H_1}(z_1, \mu) \otimes f_{j/H_2}(z_2, \mu), \end{aligned} \quad (2.9)$$

which is correct up to power corrections in q_T^2/Q^2 and $x_T^2 \Lambda_{\text{QCD}}^2$, where $x_T^2 = -x_\perp^2$ and x_\perp is the Fourier conjugate variable to q_T . The perturbative function $C_{q\bar{q} \leftarrow ij}$ is given in terms of the Wilson coefficient C_V as,

$$\begin{aligned} C_{q\bar{q} \leftarrow ij}(z_1, z_2, q_T^2, Q^2, \mu) &= |C_V(Q^2, \mu)|^2 \int d^2x_\perp e^{-iq_\perp \cdot x_\perp} \left(\frac{x_T^2 q^2}{4e^{-2\gamma_E}} \right)^{-F_{q\bar{q}}(x_T^2, \mu)} \\ &\quad \times I_{q/i}(z_1, x_T^2, \mu) I_{\bar{q}/j}(z_2, x_T^2, \mu). \end{aligned} \quad (2.10)$$

This is the form in which we have implemented the factorization formula, taking the explicit form for the functions $I_{q/i}$ and F from Ref. [124]. Since all the formula are explicitly given in a machine readable format this gives the simplest implementation method. An alternative approach would be to use Ref. [125] where a number of useful results are collected. Ref. [125] has the ambition to be more complete, since it also gives results which are relevant at N³LO, but for our purposes, i.e. NNLO, it is less useful since for some of the needed components it refers to other papers. We have checked that a full NNLO implementation based on Ref. [125] and papers referenced therein gives the same result as in Ref. [124].

The q_T spectrum for color singlet production including the complete q_T^2/Q^2 power corrections at $O(\alpha_s)$, has been presented in ref. [126]. Power corrections for the NLO inclusive cross section of Drell-Yan processes have been calculated up to fourth order in a transverse-momentum cut in Ref. [127], and up to second order for the NNLO qg -initiated channel in Ref. [128]. Therefore a full suite of power corrections at NNLO is not available, even for the simplest processes.

2.3 Hard functions

The hard functions are related to finite parts of the virtual one- and two-loop corrections to the Born process. For the case of the Drell-Yan type processes, (W, Z and γ^*) the two-loop corrections are given in Refs. [129, 130]. For the case of Higgs production in the large m_t limit the two-loop corrections are given in Refs. [130–133]. For the $V\gamma$ ($V = Z, W^\pm$) processes the finite remainders of the one-loop and two-loop form factors are given in [90], while the remainders for the $\gamma\gamma$ process are specified in Ref. [134]. For the diboson ($W^+W^-, W^\pm Z, ZZ$) processes, with the vector bosons decaying leptonically, the matrix elements up to two loops have been computed in Ref. [91]. Details of the conversion of the two-loop matrix elements in Ref. [91] to the hard functions are presented in Appendix B. We employ HandyG [135] for the numerical evaluation of multiple polylogarithms that appear in the expression of two-loop finite remainders.

2.4 Above cut contributions

A necessary ingredient for the vector boson pair calculations is the NLO calculation of the desired parton process but with one additional parton in the final state. In preparation for this paper we have implemented and improved the treatment of the $VV + \text{jet}$ process at one-loop, for the cases of $VV = W^+W^-, W^\pm Z, ZZ$. As with all NLO processes in MCFM these are included using analytic formula. Analytic results for the one-loop calculation of the $W^+W^- + 3$ parton process have been given in Ref. [136]. After simple modifications these results can also be applied to the WZ and ZZ processes. Although the results of Ref. [136] were in analytic form, considerable effort has been devoted to simplifying these results [137]. Analytic results for the one-loop calculation of the $W^+\gamma + 3$ parton process, applicable also to the $Z\gamma$ process, have been given in Ref. [30].

We have compared our one-loop results with OpenLoops 2 [89] and Recola2 [138, 139], both as a confirmation of the results and to establish timings. The comparison is performed via an extension of the C++ interface to MCFM [140], computing the interference of Born and 1-loop amplitudes using the same set of 1000 representative phase-space points with the default setup for both OpenLoops 2 (version 2.1.2) and Recola2 (version 2.2.3). Our calculations agree perfectly with those of these libraries³, with timing results shown in Table 2. Although the evaluation of this part of the full NNLO result is not the most expensive in terms of computing time, our results are in all cases faster than both Openloops 2 and Recola2.

3 Comparative study of jettiness and q_T slicing

In this section we exploit the leading logarithmic dependence on the transverse momentum cut, q_T^{cut} and jettiness cut, τ^{cut} , to define the appropriate variables to compare the two approaches. The leading logarithmic behaviour of a colour singlet cross section integrated

³For the $Z\gamma + \text{jet}$ and $WW + \text{jet}$ processes agreement is established only in the limit $m_t \rightarrow \infty$ since the top-quark contributions, that decouple in this limit, are not included in the MCFM calculation of the 1-loop amplitudes.

Parton channel	Process	$\kappa(\text{OpenLoops 2})$	$\kappa(\text{Recola2})$	$t_{MCFM}[\text{s}/1000 \text{ pts}]$
$d\bar{u} \rightarrow e^- \bar{\nu}_e \gamma g$	$W^- \gamma + \text{jet}$	31.2	23.7	0.14
$u\bar{d} \rightarrow e^+ \nu_e \gamma g$	$W^+ \gamma + \text{jet}$	29.1	24.3	0.14
$u\bar{d} \rightarrow e^+ e^- \gamma g$	$Z \gamma + \text{jet}$	24.1	15.5	0.78
$u\bar{u} \rightarrow e^- \bar{\nu}_e \mu^+ \nu_\mu g$	$W^+ W^- + \text{jet}$	17.9	12.0	0.4
$d\bar{u} \rightarrow e^- \bar{\nu}_e \mu^+ \mu^- g$	$W^- Z + \text{jet}$	7.2	5.2	0.83
$u\bar{d} \rightarrow e^+ \nu_e \mu^+ \mu^- g$	$W^+ Z + \text{jet}$	7.1	5.2	0.83
$u\bar{u} \rightarrow e^- e^+ \mu^+ \mu^- g$	$ZZ + \text{jet}$	15.8	3.8	3.6

Table 2. The relative timing of the OpenLoops 2 and Recola2 libraries, to the analytic 1-loop calculations in MCFM, for the calculation of a single partonic channel for each diboson process. The speed-up factor when using MCFM rather than a library X is denoted by $\kappa(X)$, where $\kappa(X) = t_X/t_{MCFM}$ and the timings t are established by computing results for 1000 phase-space points on an Intel Xeon E5-2650 2.60GHz CPU.

up to a small cutoff value, q_T^{cut} , is

$$\Sigma_T = \sigma_0 \exp \left[-\frac{\alpha_s C_F}{2\pi} \ln^2((q_T^{\text{cut}})^2/Q^2) \right] = \sigma_0 \exp \left[-\frac{2\alpha_s C_F}{\pi} \ln^2(q_T^{\text{cut}}/Q) \right], \quad (3.1)$$

where σ_0 is the Born level cross section. The corresponding leading log formula for zero-jettiness integrated up to a cut of value τ^{cut} is,

$$\Sigma_\tau = \sigma_0 \exp \left[-\frac{\alpha_s C_F}{\pi} \ln^2 \frac{\tau^{\text{cut}}}{Q} \right]. \quad (3.2)$$

A simple derivation of these two formulas at order α_s is given in Appendix A.

The resources needed for a computation of a given accuracy is dominated by the calculation of the above-cut contribution. Comparing Eqs. (3.1) and (3.2) one therefore expects a similar size for the contribution coming from the above cut region when the values of τ^{cut} and q_T^{cut} are related by [141],

$$\frac{\tau^{\text{cut}}}{Q} \simeq \left(\frac{q_T^{\text{cut}}}{Q} \right)^{\sqrt{2}}. \quad (3.3)$$

We therefore define the following two dimensionless quantities to encapsulate the slicing dependence of the results,

$$\epsilon_T = q_T^{\text{cut}}/Q, \quad (3.4)$$

and

$$\epsilon_\tau = (\tau^{\text{cut}}/Q)^{\frac{1}{\sqrt{2}}}. \quad (3.5)$$

The computational burden is then expected to be very similar for equal values of ϵ_T and ϵ_τ and therefore we will compare the two schemes at the same values of ϵ_T and ϵ_τ . Although this argument is only made at the level of leading logarithms, we will see later (c.f. Table 5 in Section 3.4) that it is indeed supported even at NNLO for the operating values of ϵ_τ and ϵ_T that we choose. We note that all the results presented in this paper are obtained using a modified version of the MCFM-9.0 code, thus allowing the computation of cross sections

at multiple values of ϵ_T or ϵ_τ in one run [6]. In order to present a fair comparison between the two approaches we generate the phase space in an identical way in both cases, one that has not been optimized for either.

3.1 Processes and cuts

For simplicity, and in order to avoid issues associated with the application of fiducial cuts in 2-body decays [92, 93], we present results for inclusive Z , W^\pm , H , ZH and $W^\pm H$ production. Decays of the W , Z and H bosons are not included and no cuts are applied.

The remaining processes we compute are:

$$\begin{aligned}
pp &\rightarrow \gamma\gamma \\
pp &\rightarrow e^-e^+\gamma & Z\gamma \\
pp &\rightarrow e^-\bar{\nu}_e\gamma & W^-\gamma \\
pp &\rightarrow \nu_e e^+\gamma & W^+\gamma \\
pp &\rightarrow e^-\mu^+\bar{\nu}_e\nu_\mu & W^-W^+ \\
pp &\rightarrow e^-e^+\mu^-\mu^+ & ZZ \\
pp &\rightarrow e^-\bar{\nu}_e\mu^-\mu^+ & W^-Z \\
pp &\rightarrow \nu_e e^+\mu^-\mu^+ & W^+Z
\end{aligned} \tag{3.6}$$

As indicated, these processes include a full set of contributing Feynman diagrams and are not limited to those containing on-shell W or Z propagators. We will, however, often use these names as shorthand in the remainder of the paper. The calculation of these processes includes the application of cuts to identify photons and leptons. In order to provide an additional cross-check we have adopted the sets of cuts used in Ref. [24] for the processes in Eq. (3.6). The cuts for the processes are given in Tables 7–10 of that reference. For the convenience of the reader all the cuts that we use for the various processes are given in appendix C. We choose a common renormalization and factorization scale μ that, however, depends upon the process as follows: $\mu = m_H$ (H), $\mu = m_V$ ($V = W$ or Z), $\mu = m_{VH}$ (VH), $\mu = m_{\gamma\gamma}$ ($\gamma\gamma$), $\mu = \sqrt{m_V^2 + (p_T^\gamma)^2}$ ($V\gamma$), $\mu = (m_{V_1} + m_{V_2})/2$ (V_1V_2).

3.2 Input parameters

Most parameters are specified in Table 3, where for generality we have identified values in the complex mass scheme [142]. However, for the calculation of the inclusive cross-sections (i.e. Z , W^\pm , H , ZH and $W^\pm H$ production) described in section 3.1 all parameters are kept real by setting $\Gamma_Z = \Gamma_W = \Gamma_H = 0$.

For W^\pm production we use a CKM matrix that employs the 2016 PDG values [143]:

$$\begin{pmatrix} V_{ud} & V_{us} & V_{ub} \\ V_{cd} & V_{cs} & V_{cb} \end{pmatrix} = \begin{pmatrix} 0.97417 & 0.2248 & 0.00409 \\ 0.22 & 0.995 & 0.0405 \end{pmatrix} \tag{3.7}$$

In all other processes we use a diagonal CKM matrix. We use $n_f = 5$ flavours of massless partons throughout, except for the W^-W^+ process that uses $n_f = 4$ to eliminate contributions at NNLO from final states such as $W^-W^+b\bar{b}$ (that are considered a part of $t\bar{t}$

M_W	80.385 GeV	Γ_W	2.0854 GeV
M_Z	91.1876 GeV	Γ_Z	2.4952 GeV
G_μ	$1.166390 \times 10^{-5} \text{ GeV}^{-2}$		
m_t	173.2 GeV	m_h	125 GeV
$m_W^2 = M_W^2 - iM_W\Gamma_W$	$(6461.748225 - 167.634879 i) \text{ GeV}^2$		
$m_Z^2 = M_Z^2 - iM_Z\Gamma_Z$	$(8315.17839376 - 227.53129952 i) \text{ GeV}^2$		
$\cos^2 \theta_W = m_W^2/m_Z^2$	$(0.7770725897054007 + 0.001103218322282256 i)$		
$\alpha = \frac{\sqrt{2}G_\mu}{\pi} M_W^2 (1 - \frac{M_W^2}{M_Z^2})$	$7.56246890198475 \times 10^{-3}$ giving $1/\alpha \approx 132.23 \dots$		

Table 3. Input and derived parameters used for our numerical estimates.

production and subsequent decay). For the $W^\pm H$ and ZH processes, diagrams in which the Higgs boson couples directly to a top quark loop are computed in the effective theory that is valid in the large m_t limit. Contributions from a massive top quark are neglected in the virtual 2-loop matrix elements for all processes, and also throughout the calculation of NNLO corrections to the W^-W^+ and $Z\gamma$ processes.

All calculations are performed at $\sqrt{s} = 13 \text{ TeV}$ and we use the NNPDF3.0 set of parton distribution functions [144], with the set matched to the order of the calculation and the number of quark flavours.

3.3 NLO

We first provide a set of illustrative results by computing results at NLO accuracy, using both non-local slicing methods. At this order we can also compute benchmark results directly in MCFM using the subtraction method[145] in the dipole formulation [146].

3.3.1 Inclusive processes

The NLO results for inclusive production are shown in Fig. 1 ($2 \rightarrow 1$ processes) and Fig. 2 ($2 \rightarrow 2$ associated Higgs production processes). For WH production we show the result for the sum of the two W charges, $\sigma(W^\pm H) = \sigma(W^+ H) + \sigma(W^- H)$. The result for the NLO cross section is computed as a function of ϵ_T for 0-jettiness, c.f. Eq. (3.5), and as a function of ϵ_T for q_T -slicing, c.f. Eq. (3.4). Since the value of the cutoff used to present the NNLO results in Ref. [24] is $\epsilon_T = q_T^{\text{cut}}/Q = 0.15\%$ we perform the calculation at values of ϵ with this as a lower bound. We note that setting $\epsilon_T = 0.15\%$ corresponds to $\tau^{\text{cut}}/Q \approx 10^{-4}$, c.f. Eq. (3.5).

The results from the non-local slicing schemes are compared to those of MCFM dipole-subtraction calculations, which also all agree fully with the results reported in Table 6 of Ref. [24]. A fit to the results at fixed values of ϵ_T and ϵ_r is performed using the form,

$$\sigma^{NLO}(\epsilon) = a_0 + a_1 \epsilon^r \log \epsilon^r + a_2 \epsilon^r, \quad (3.8)$$

where $r = 2$ (q_T) and $r = \sqrt{2}$ (0-jettiness) effectively undoes the rescaling introduced in Eq. (3.5). This fit form anticipates the effect of possible power corrections to the factoriza-

tion theorems used in obtaining the below-cut contribution (quadratic for q_T and linear for 0-jettiness) but here we only use this fit to guide the eye.

In all cases the results from the non-local slicing calculations approach the known cross sections as the cutoff approaches zero. For H , $W^\pm H$ and ZH production the residual difference from the known result is smaller for q_T than 0-jettiness slicing, for results at equal values of ϵ_T and ϵ_τ . For the Z and W^\pm processes the relative ordering is reversed. We note that all the points in these plots have been obtained by running the MCFM code with a target Monte Carlo precision that is the same for 0-jettiness and q_T slicing, so that the statistical errors on data points of equal ϵ_T and ϵ_τ are similar. The running time of the code to reach this level of precision is essentially the same for the two non-local slicing methods, thereby providing an indirect confirmation of the scaling behavior introduced in Eq. (3.3).

3.3.2 Diboson production

Corresponding results for processes involving a photon are shown in Fig. 3 and, for the remaining diboson cases, in Fig. 4. Note that here, since the definition of these processes includes the application of fiducial cuts, we have fixed $r = 1$ in Eq. (3.8) for q_T -slicing to anticipate the presence of linear power corrections. In Fig. 3, processes in which a final-state photon is observed, the approach to the known result is almost identical for 0-jettiness and q_T slicing. This is also true for the ZZ process, but for the other diboson processes q_T slicing is much closer to the correct result than 0-jettiness for equal values of ϵ_T and ϵ_τ .

For the diphoton case we have also investigated the use of “product cuts”, as advocated in Ref. [93], rather than the asymmetric cuts that are our default choice. Since we already observe no pathology in the asymmetric cut results of Fig. 3 the corresponding results for product cuts are qualitatively similar and we do not show them separately here. Since the study of Ref. [93] is motivated by sensitivity specifically arising from the 2-body decay of a parent particle this is expected; the rapidly falling p_T spectrum in the continuum $pp \rightarrow \gamma\gamma$ case mitigates any similar issue here.

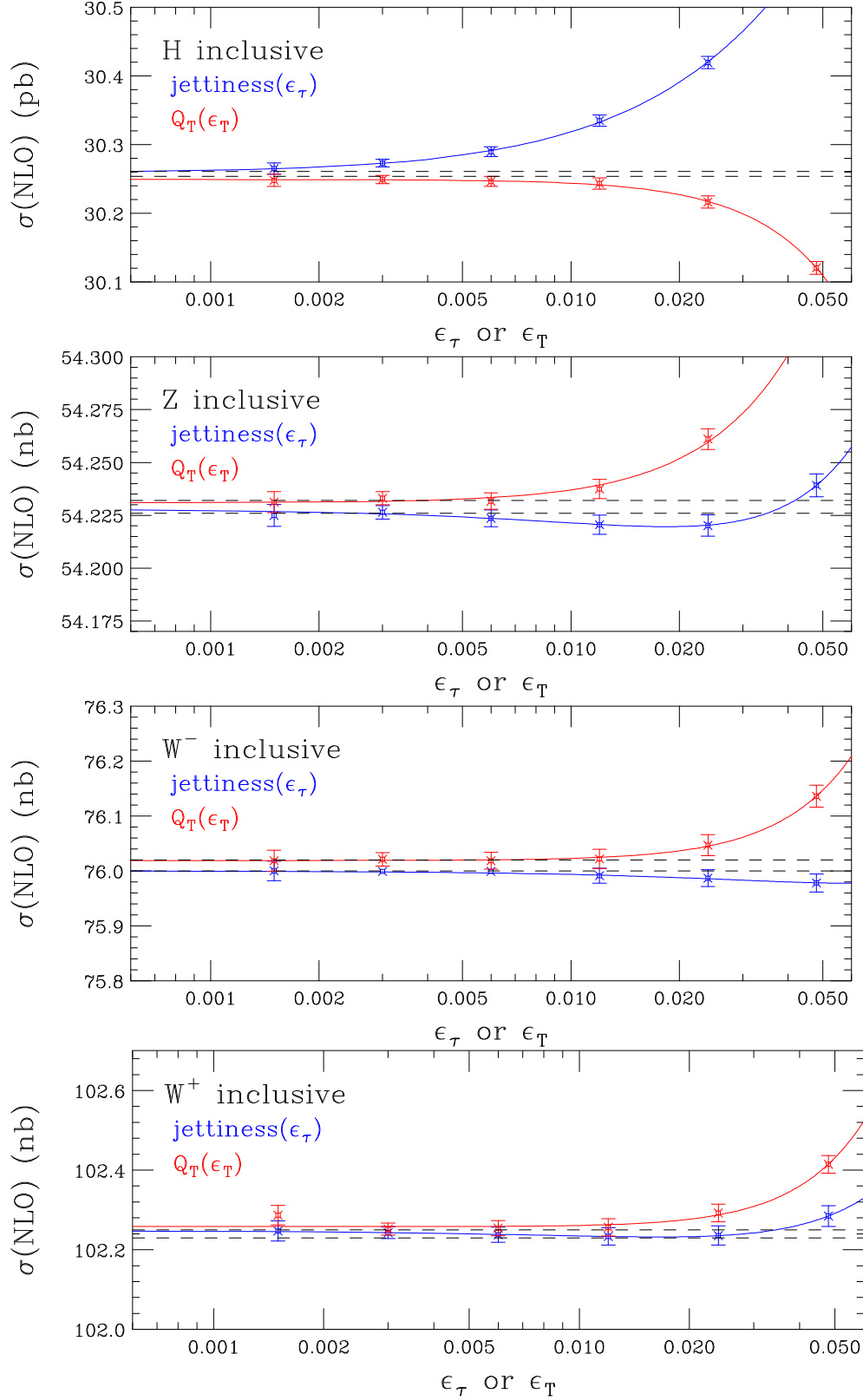


Figure 1. Dependence of NLO cross section for $pp \rightarrow h$, $pp \rightarrow Z$, $pp \rightarrow W^-$ and $pp \rightarrow W^+$ processes on choice of slicing cut, for both 0-jettiness and q_T -slicing. The uncertainty band of the exact result, computed with MCFM using dipole subtraction, is shown as the dashed lines.

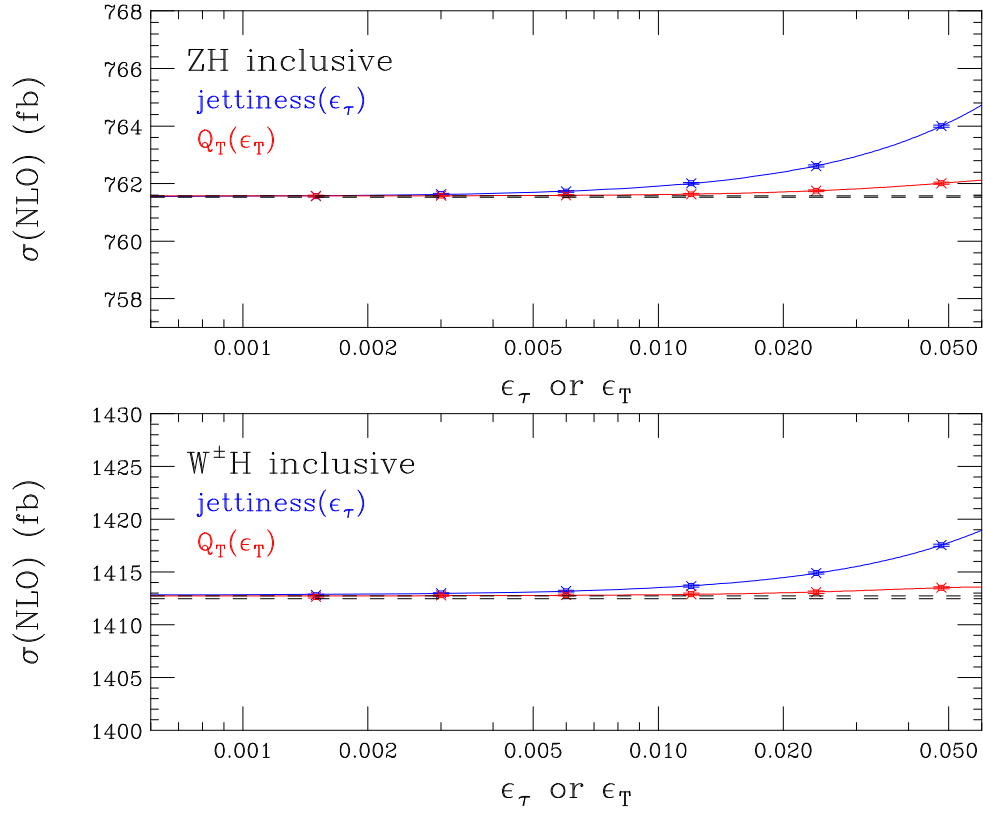


Figure 2. Dependence of NLO cross section for inclusive ZH and $W^\pm H$ (sum of $W^+ H$ and $W^- H$) processes on choice of slicing cut, for both 0-jettiness and q_T -slicing. The uncertainty band of the exact result, computed with MCFM using dipole subtraction, is shown as the dashed lines.

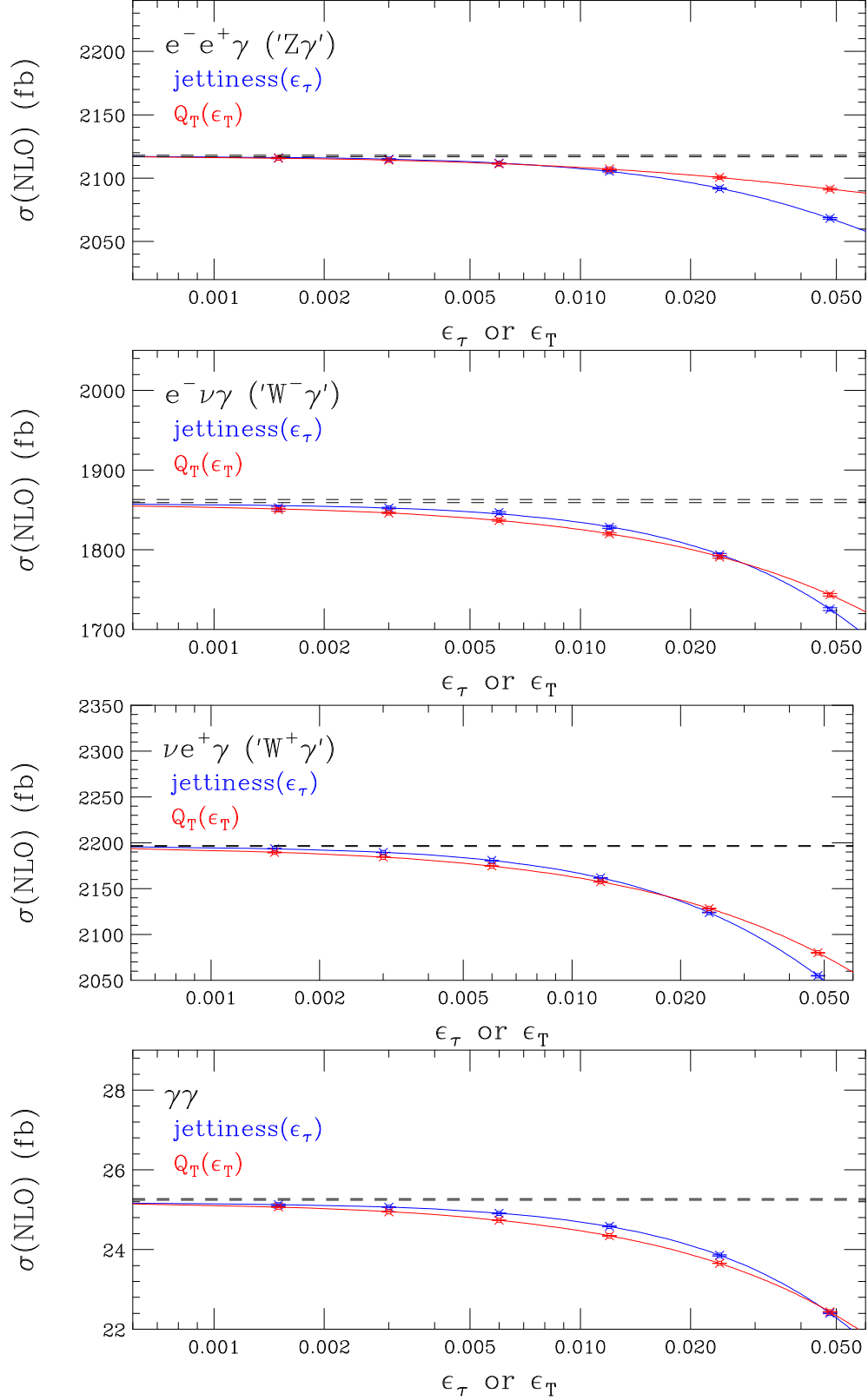


Figure 3. Dependence of NLO cross section for $Z\gamma$, $W^-\gamma$, $W^+\gamma$ and $\gamma\gamma$ processes on choice of slicing cut, for both 0-jettiness and q_T -slicing. The uncertainty band of the exact result, computed with MCFM using dipole subtraction, is shown as the dashed lines.

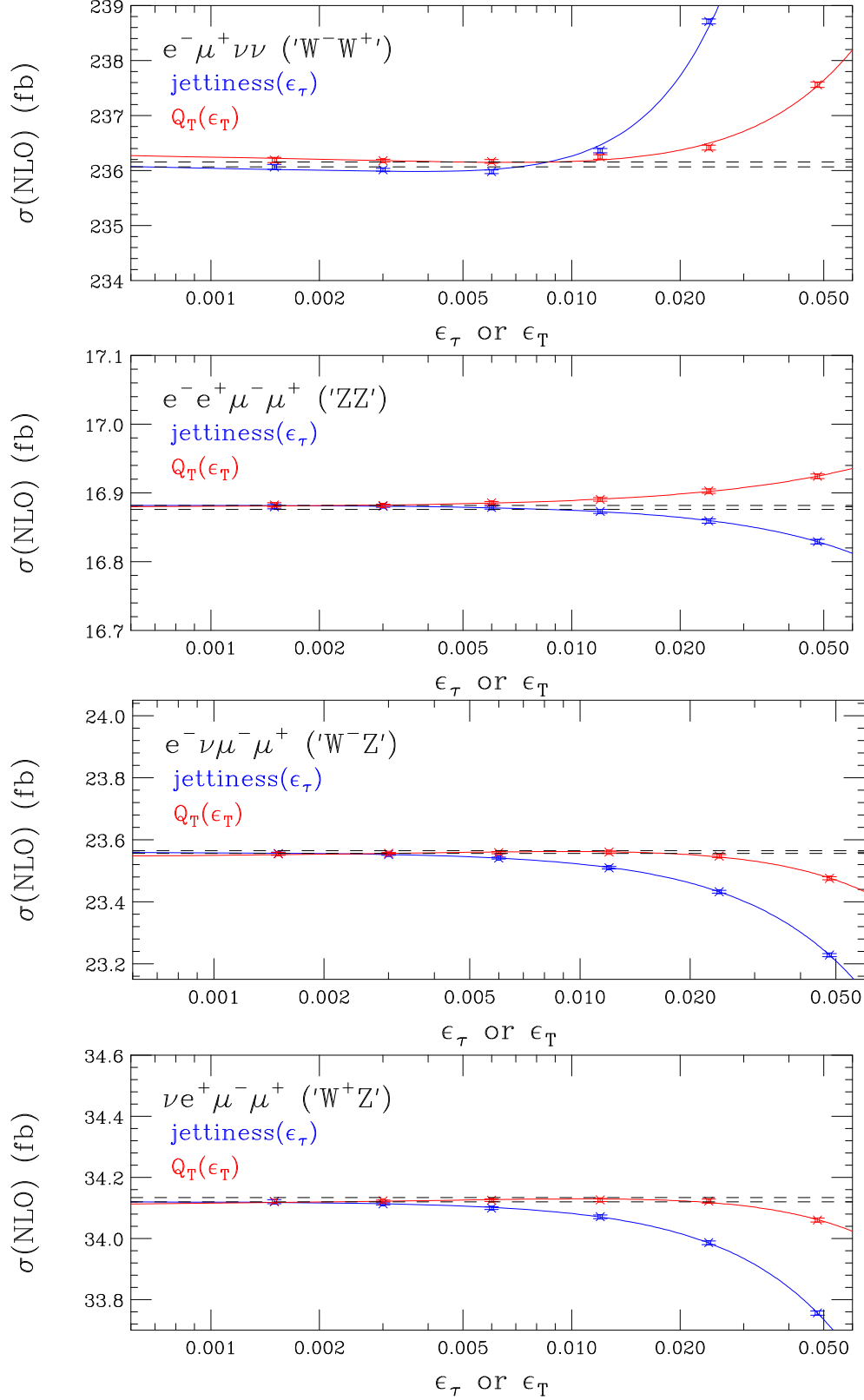


Figure 4. Dependence of NLO cross section for $pp \rightarrow WW$, $pp \rightarrow ZZ$, $pp \rightarrow W^- Z$ and $pp \rightarrow W^+ Z$ processes on choice of slicing cut, for both 0-jettiness and q_T -slicing. Dashed line is the NLO result computed with MCFM using dipole subtraction.

Process	target			MCFM		
	σ_{NLO^*}	σ_{NNLO}	δ_{NNLO}	σ_{NNLO}	δ_{NNLO}	
$pp \rightarrow H$	29.78(0)	39.93(3)	10.15(3)	39.91(5)	10.13(5)	nb
$pp \rightarrow Z$	56.41(0)	55.99(3)	-0.42(3)	56.03(3)	-0.38(3)	nb
$pp \rightarrow W^-$	79.09(0)	78.33(8)	-0.76(8)	78.41(6)	-0.68(6)	nb
$pp \rightarrow W^+$	106.2(0)	105.8(1)	-0.4(1)	105.8(1)	-0.4(1)	nb
$pp \rightarrow \gamma\gamma$	25.61(0)	40.28(30)	14.67(30)	40.19(20)	14.58(20)	pb
$pp \rightarrow e^-e^+\gamma$	2194(0)	2316(5)	122(5)	2315(5)	121(5)	pb
$pp \rightarrow e^-\bar{\nu}_e\gamma$	1902(0)	2256(15)	354(15)	2251(2)	349(2)	pb
$pp \rightarrow e^+\nu_e\gamma$	2242(0)	2671(35)	429(35)	2675(2)	433(2)	pb
$pp \rightarrow e^-\mu^-e^+\mu^+$	17.29(0)	20.30(1)	3.01(1)	20.30(2)	3.01(2)	fb
$pp \rightarrow e^-\mu^+\nu_\mu\bar{\nu}_e$	243.7(1)	264.6(2)	20.9(3)	264.9(9)	21.2(8)	fb
$pp \rightarrow e^-\mu^-e^+\bar{\nu}_\mu$	23.94(1)	26.17(2)	2.23(3)	26.18(3)	2.24(2)	fb
$pp \rightarrow e^-e^+\mu^+\nu_\mu$	34.62(1)	37.74(4)	3.12(5)	37.78(4)	3.16(3)	fb
$pp \rightarrow ZH$	780.0(4)	846.7(5)	66.7(6)	847.3(7)	67.3(6)	fb
$pp \rightarrow W^\pm H$	1446.5(7)	1476.1(7)	29.6(10)	1476.7(8)	30.2(4)	fb

Table 4. NLO results, computed using MCFM with NNLO PDFs (denoted σ_{NLO^*}), total NNLO cross sections from `vh@nnlo` ($W^\pm H$ and ZH only) and MATRIX (remaining processes, using the extrapolated result from Table 6 of Ref. [24]) and the target NNLO coefficients (δ_{NNLO} , with $\delta_{NNLO} = \sigma_{NNLO} - \sigma_{NLO^*}$). The result of the MCFM calculation (0-jettiness, fit result b_0 from Eq. (3.9)) is shown in the final column.

3.4 NNLO

Having established the format and pattern of results at NLO, we now turn our attention to NNLO. At this order we may compare with the results of Ref. [24] for most processes and for the remaining $W^\pm H$ and ZH processes with the code `vh@nnlo` [147, 148]. To focus more closely on the behaviour of the calculation at this order we will show results not for the total NNLO cross section, but for the $\mathcal{O}(\alpha_s^2)$ contribution that enters at this order. In order to extract benchmark predictions for this quantity from Refs. [24, 147, 148] we have computed the NLO cross section for each process using NNLO PDFs (denoted σ_{NLO^*} in the table) and subtracted these values from the corresponding NNLO results. To compare with the MATRIX cross sections this method is used to obtain results for $\epsilon_T = 0.15\%$ and after their extrapolation procedure. The target NNLO corrections for comparison purposes are shown in Table 4, as well as the results of the NNLO calculations using MCFM.

As at NLO, for each process we have used a target numerical precision for the calculation of each process in order to compare the jettiness and q_T slicing methods. The actual precisions attained and the corresponding CPU times required, for the operating points $\epsilon_\tau = 0.15\%$ and $\epsilon_T = 0.15\%$, are shown in Table 5. The time required for each slicing method to reach a similar level of precision is very close for all processes, suggesting that the scaling introduced in Eq. (3.5) remains valid at NNLO for these values of the slicing parameters. The timings for the processes $pp \rightarrow e^-\bar{\nu}_e\gamma$ and $pp \rightarrow e^+\nu_e\gamma$ differ the most, suggesting that the presence of an identified photon in these processes may alter the scaling somewhat (at least, under these cuts). However, the timings are still not dissimilar, especially given the

Process	method	rel. unc. on δ_{NNLO}	time (CPU days)
$pp \rightarrow H$	jettiness	0.0029	54.7
	q_T	0.0029	54.7
$pp \rightarrow Z$	jettiness	0.045	356
	q_T	0.039	364
$pp \rightarrow W^-$	jettiness	0.029	274
	q_T	0.029	277
$pp \rightarrow W^+$	jettiness	0.084	238
	q_T	0.086	275
$pp \rightarrow \gamma\gamma$	jettiness	0.0090	0.77
	q_T	0.0079	0.89
$pp \rightarrow e^-e^+\gamma$	jettiness	0.023	340
	q_T	0.024	330
$pp \rightarrow e^-\bar{\nu}_e\gamma$	jettiness	0.0032	310
	q_T	0.0029	220
$pp \rightarrow e^+\nu_e\gamma$	jettiness	0.0029	317
	q_T	0.0028	231
$pp \rightarrow e^-\mu^-e^+\mu^+$	jettiness	0.0040	317
	q_T	0.0039	358
$pp \rightarrow e^-\mu^+\nu_\mu\bar{\nu}_e$	jettiness	0.012	431
	q_T	0.013	395
$pp \rightarrow e^-\mu^-e^+\bar{\nu}_\mu$	jettiness	0.0046	343
	q_T	0.0053	323
$pp \rightarrow e^-e^+\mu^+\nu_\mu$	jettiness	0.0048	441
	q_T	0.0052	359
$pp \rightarrow ZH$	jettiness	0.0047	87.3
	q_T	0.0046	89.9
$pp \rightarrow W^\pm H$	jettiness	0.021	47.5
	q_T	0.019	46.8

Table 5. Summary of run parameters for the NNLO calculations presented in this paper. For each process, the table indicates the relative uncertainty on the NNLO coefficient (δ_{NNLO}) that is computed (for the lowest values of ϵ_τ and ϵ_T shown in this paper), as well as the time taken (in CPU days) to perform each calculation.

computational effort that must be employed for even small gains in numerical precision at this point ($\sim 0.3\%$ on the NNLO coefficient).

3.4.1 Inclusive production

Results for the NNLO corrections to the inclusive calculations considered in this paper are shown in Figs. 5 and 6. As at NLO we also show a fit to the data points, but this time using a form appropriate for power corrections that could be present at NNLO,

$$\sigma^{NNLO}(\epsilon) = b_0 + b_1\epsilon^r \log^3 \epsilon^r + b_2\epsilon^r \log^2 \epsilon^r + b_3\epsilon^r. \quad (3.9)$$

For the $2 \rightarrow 1$ processes shown in Fig. 5 we also indicate the MATRIX result for $\epsilon_T = 0.15\%$ and the extrapolated result, as given in table 4, from the same calculation. For the associated Higgs production processes we also show the `vh0nnlo` results in Fig. 6.

The results from the two non-local subtraction schemes are in excellent agreement in the limit $\epsilon \rightarrow 0$, and in the case of the $2 \rightarrow 1$ processes, also match those extracted from Ref. [24]. The approach to this limit differs substantially between the two subtraction schemes; results in the q_T scheme are much closer to the asymptotic value across the range while, in contrast, 0-jettiness suffers from much larger corrections at finite values of ϵ_T .

3.4.2 Diboson production

Results for the NNLO corrections to the diboson processes considered in this paper are shown in Figs. 7 and 8, together with the benchmark results from table 4 (extracted from Ref. [24]). For the newly-included processes in MCFM, shown in Fig. 8, we note the excellent agreement with the previous calculations reported by the MATRIX collaboration.

As at NLO, for the processes with an identified photon in the final state the approach to the asymptotic limit is similar for both q_T and 0-jettiness subtraction. This indicates that power corrections to the factorization theorems underlying Eqs. (2.6) and (2.9) are affected by the requirement of photon isolation in a similar way. For the other diboson processes 0-jettiness suffers from much larger power corrections than q_T subtraction.

3.5 Comparison with Ref. [1]

In Ref. [1] Heinrich et al have produced NNLO predictions for Z -boson pair production using the 0-jettiness subtraction method to isolate the doubly unresolved region. Note that in Ref. [1] the Z 's are considered on-shell, and consequently there is no need to introduce the complex mass scheme. Adjusting our input parameters accordingly, we obtain the results shown in Table 6. Excellent agreement with the earlier calculation is observed.

	σ_{LO} [pb]	σ_{NLO} [pb]	σ_{NNLO} [pb]
Ref. [1]	9.845	14.100	$16.69(0)^{+3.1\%}_{-2.8\%}$
MCFM	9.856	14.114	$16.68(1)^{+3.2\%}_{-2.7\%}$

Table 6. Comparison with the on-shell ZZ results using NNPDF3.0 from Ref. [1]. The quoted uncertainties at NNLO correspond to those obtained by scale variation according to the procedure described in this reference.

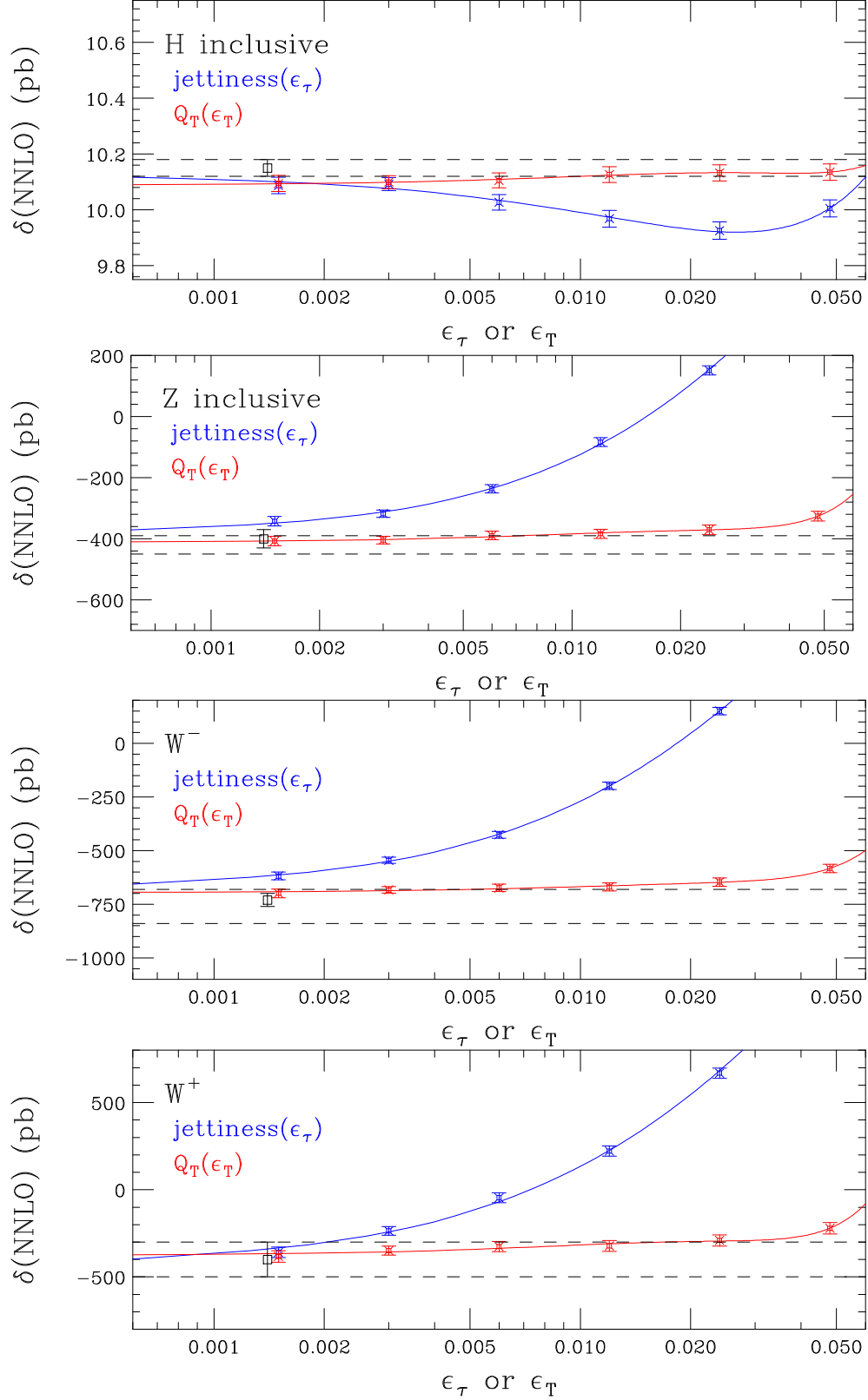


Figure 5. Dependence of NNLO coefficient for inclusive H , Z , W^- and W^+ processes on choice of slicing cut, for both 0-jettiness and q_T -slicing. The MATRIX result for $q_T^{\text{cut}} = 0.15\%$, Ref. [24] corresponds to the square black point (slightly offset for visibility) and the uncertainty band of the extrapolated MATRIX result is shown as the dashed lines.

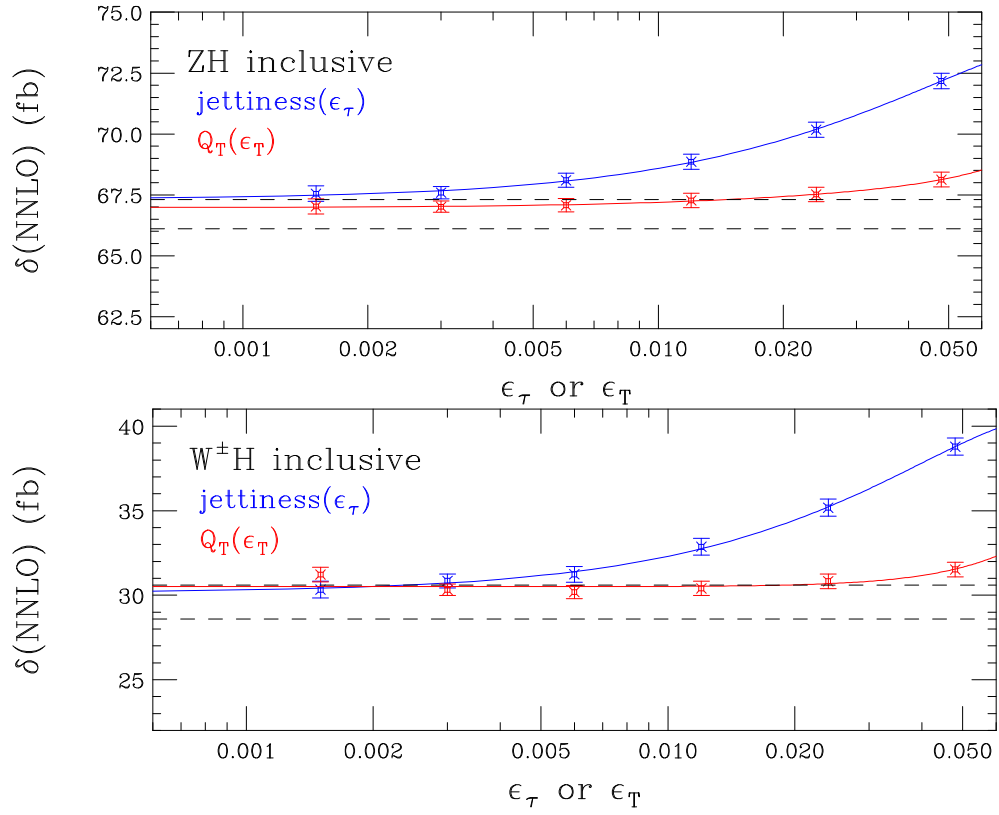


Figure 6. Dependence of NNLO coefficient for inclusive ZH and $W^\pm H$ (sum of W^+H and W^-H) processes on choice of slicing cut, for both 0-jettiness and q_T -slicing. The dashed lines represent the uncertainty band of the `vh@nnlo` result [147, 148].

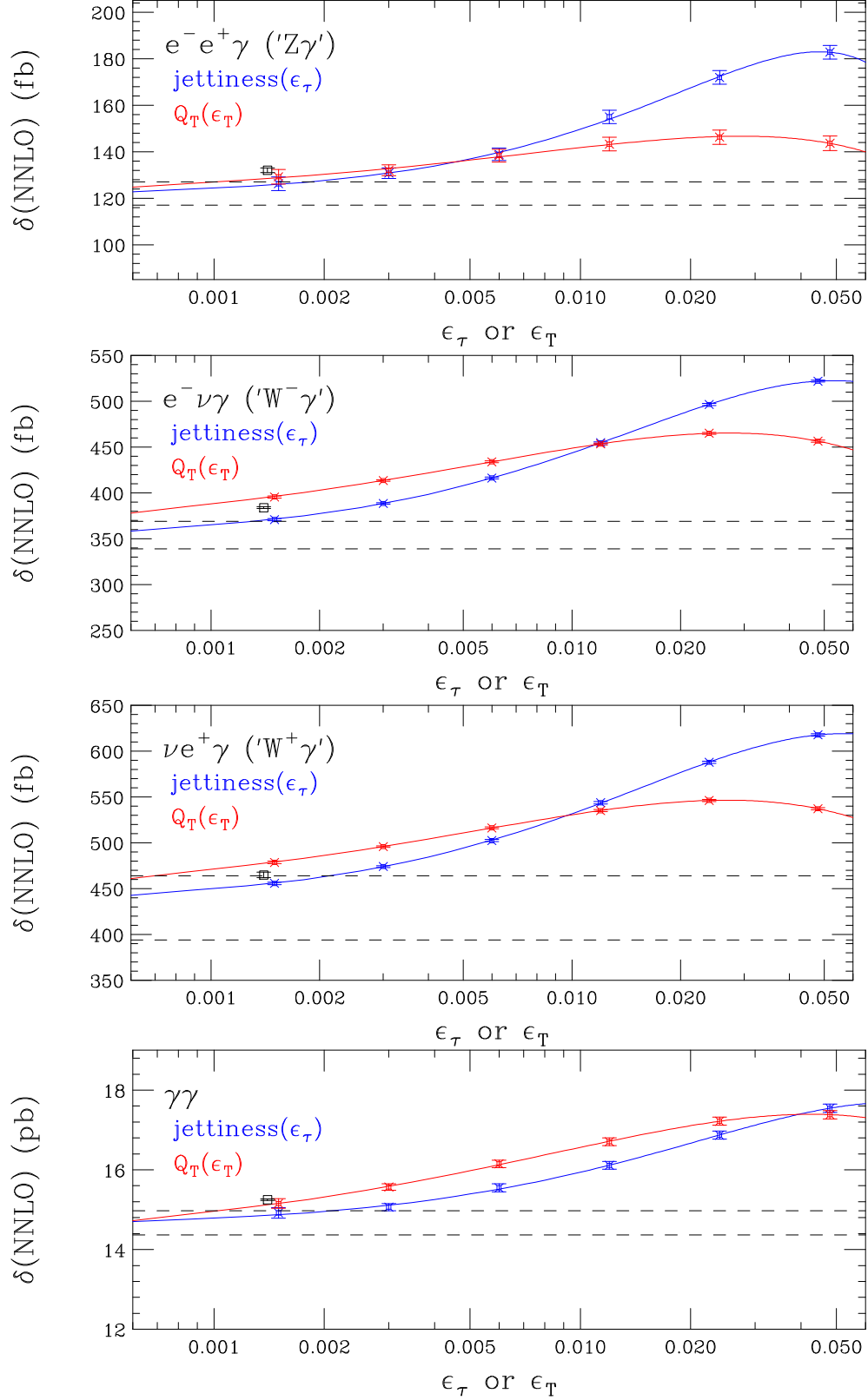


Figure 7. Dependence of NNLO coefficient for $Z\gamma$, $W^-\gamma$, $W^+\gamma$ and $\gamma\gamma$ processes on choice of slicing cut, for both 0-jettiness and q_T -slicing. The MATRIX result for $q_T^{\text{cut}} = 0.15\%$, Ref. [24] corresponds to the square black point (slightly offset for visibility) and the uncertainty band of the extrapolated MATRIX result is shown as the dashed lines.

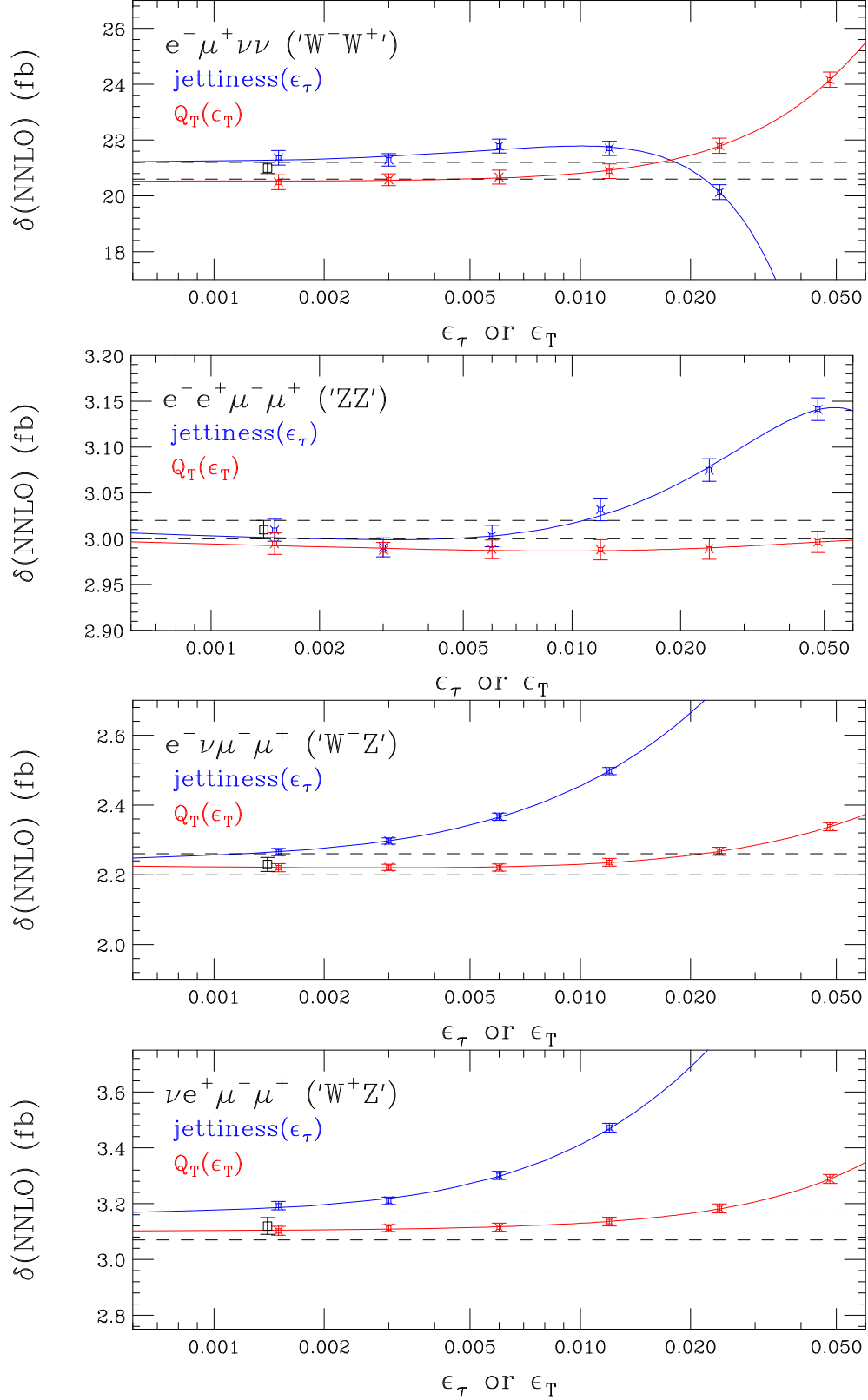


Figure 8. Dependence of NNLO coefficient for $pp \rightarrow WW$, $pp \rightarrow ZZ$, $pp \rightarrow W^- Z$ and $pp \rightarrow W^+ Z$ processes on choice of slicing cut, for both 0-jettiness and q_T -slicing. The MATRIX result for $q_T^{\text{cut}} = 0.15\%$, Ref. [24] corresponds to the square black point (slightly offset for visibility) and the uncertainty band of the extrapolated MATRIX result is shown as the dashed lines.

4 Conclusion

Our intent in the current paper has been to increase the range of processes which are available in the MCFM package at NNLO in QCD. Specifically we have added the processes, W^+W^- , $W^\pm Z$ and ZZ , with leptonic decays of the W and Z bosons included. As well as its extensive range of processes available at NLO using dipole subtraction, MCFM now includes a wide range of processes at NNLO. Representative results for the processes that are now included at this order have been presented in Table 4. We have implemented two different slicing methods for the calculation of the NNLO QCD corrections to processes with colour singlet final states. Both methods use global variables to isolate the region of phase space with soft and collinear emission.

The jettiness method divides the phase space on the basis of the zero-jettiness, defined in Eq. (2.5) whereas the q_T method divides the phase space on the basis of the total transverse momentum of the colour singlet particles. We find that the q_T -slicing method appears to be subject to smaller power corrections in most cases, although in certain cases ($W^\pm\gamma$, $Z\gamma$, $\gamma\gamma$ at NNLO) the size of the power corrections is similar, or even slightly smaller for jettiness. We note that all these processes involve photon isolation cuts.

Since there is a well-developed literature on the summation of logarithms of transverse momentum the q_T -slicing method is easily extended to perform resummation of logarithms of q_T . For the moment the application of the q_T -slicing method to coloured final states at NNLO has been limited to the case of heavy-quark production [64, 65, 83]. The extension to processes in which a massless parton is present in the final state is not straightforward, although there are encouraging signs at NLO using a q_T surrogate, based on the k_T jet algorithm [149]. Despite the larger power corrections, which tend to disfavour the jettiness slicing method, we note that the jettiness subtraction method already has the proven ability to deal with coloured final states, such as $W + \text{jet}$, $Z + \text{jet}$ and $H + \text{jet}$. Results for these processes have already been presented with MCFM.

We have provided a detailed comparison of the two non-local subtraction methods in a way that they are directly comparable. In this paper we have avoided as much as possible the imposition of cuts, because of the influence that injudicious choices of cuts can have on the power corrections. Resummation, by reducing the sensitivity to the low q_T region, has the benefit that it circumvents the additional power corrections which can occur in the presence of some fiducial cuts [92, 93]. The calculations we have presented provide the basis for future extensions of MCFM that include q_T resummation for diboson processes, extending the work in Refs. [96, 97].

Acknowledgments We would like to thank Giuseppe de Laurentis for assistance simplifying one-loop matrix elements. RKE thanks Gavin Salam for useful discussions. This manuscript has been authored by Fermi Research Alliance, LLC under Contract No. DE-AC02-07CH11359 with the U.S. Department of Energy, Office of Science, Office of High Energy Physics. The numerical calculations reported in this paper were performed using the Wilson High-Performance Computing Facility at Fermilab.

A Leading log behaviour of colour singlet production cross section

For simplicity, we shall consider the simple Drell-Yan process in leading order, although the discussion will apply *mutatis mutandis* to all colour singlet final states. We follow closely the discussion of ref. [150]. The lowest order cross section has the form

$$\sigma(\hat{s}, Q^2) = \sigma_0 \delta(1 - z), \quad z = Q^2/\hat{s}, \quad \sigma_0 = \frac{4\alpha\pi^2}{N\hat{s}}. \quad (\text{A.1})$$

The invariant Drell-Yan cross section with the emission of one gluon of momentum k is,

$$\begin{aligned} \frac{\pi k^0 d\sigma}{d^3k} &= \sigma_0 \int dx_1 dx_2 [f(x_1)f(x_2) + (1 \leftrightarrow 2)] \\ &\times \frac{\alpha_s C_F}{2\pi} \left(\frac{(\hat{s} + \hat{t})^2 + (\hat{s} + \hat{u})^2}{\hat{t}\hat{u}} \right) \delta(\hat{s} + \hat{t} + \hat{u} - Q^2), \end{aligned} \quad (\text{A.2})$$

where $\hat{s} = 2p_1 \cdot p_2$, $\hat{t} = -2p_1 \cdot k$, $\hat{u} = -2p_2 \cdot k$ and k is the gluon momentum. Taking the gluon momentum to be $k = \alpha p_1 + \beta p_2 + \vec{k}_T$ the invariant gluon momentum integral becomes,

$$\frac{d^3k}{k^0} = d\alpha d\beta d^2\vec{k}_T \delta(\alpha\beta - \frac{\vec{k}_T^2}{\hat{s}}). \quad (\text{A.3})$$

The parton cross section for fixed virtual photon transverse momentum q_T is,

$$\begin{aligned} \frac{1}{\hat{\sigma}_0} \frac{d\sigma}{dq_T^2} &= d\alpha d\beta \delta(\alpha\beta - \frac{\vec{Q}_T^2}{\hat{s}}) \delta(\hat{s}(1 - \alpha - \beta) - Q^2) \\ &\times \frac{\alpha_s C_F}{2\pi} \left[\frac{(1 - \alpha)^2 + (1 - \beta)^2}{\alpha\beta} \right]. \end{aligned} \quad (\text{A.4})$$

To eliminate the delta functions in these expressions it is useful to take moments with respect to $\rho = Q^2/\hat{s}$ of the partonic cross section,

$$F_n(q_T^2/s) = \frac{1}{\hat{\sigma}_0} \int_0^1 d\rho \rho^{n+1} \frac{d\hat{\sigma}}{dq_T^2}. \quad (\text{A.5})$$

In the limit $q_T \rightarrow 0$ (ignoring powers of α, β in the numerator),

$$F_n(q_T^2/\hat{s}) = \frac{\alpha_s C_F}{\pi} \frac{1}{q_T^2} \int_{q_T^2/\hat{s}} \frac{d\alpha}{\alpha} \sim -\frac{\alpha_s C_F}{\pi} \frac{\hat{s}}{q_T^2} \ln \left(\frac{q_T^2}{\hat{s}} \right). \quad (\text{A.6})$$

To explicitly exhibit the double logarithms we define,

$$\Sigma(q_T^{cut}/\hat{s}) = \int_0^{q_T^{cut2}} dq_T^2 F_n(q_T^2/\hat{s}). \quad (\text{A.7})$$

Integrating over q_T up to q_T^{cut} and cancelling IR singularities by inclusion of the virtual diagrams gives,

$$\Sigma_T = \sigma_0 \left[1 - \frac{\alpha_s C_F}{2\pi} \ln^2((q_T^{cut})^2/Q^2) \right] = \sigma_0 \left[1 - \frac{2\alpha_s C_F}{\pi} \ln^2(q_T^{cut}/Q) \right], \quad (\text{A.8})$$

the order α_s expansion of Eq. (3.1).

This should be compared with the jettiness calculation,

$$F_n(\tau/\sqrt{\hat{s}}) = \frac{\alpha_s C_F}{\pi} \int \frac{d\alpha}{\alpha} \int \frac{d\beta}{\beta} \left[\theta(\alpha - \beta) \delta(\beta - \tau/\sqrt{\hat{s}}) + \theta(\beta - \alpha) \delta(\alpha - \tau/\sqrt{\hat{s}}) \right] \quad (\text{A.9})$$

$$= \frac{\alpha_s C_F}{\pi} \frac{\sqrt{\hat{s}}}{\tau} \left[\int_{\tau/\sqrt{\hat{s}}}^1 \frac{d\alpha}{\alpha} + \int_{\tau/\sqrt{\hat{s}}}^1 \frac{d\beta}{\beta} \right] \quad (\text{A.10})$$

$$= -\frac{2\alpha_s C_F}{\pi} \frac{\sqrt{\hat{s}}}{\tau} \ln \frac{\tau}{\sqrt{\hat{s}}}. \quad (\text{A.11})$$

Integrating over τ up to τ^{cut} and cancelling IR singularities at $\tau = 0$ by inclusion of the virtual diagrams gives,

$$\Sigma_\tau = \sigma_0 \left[1 - \frac{\alpha_s C_F}{\pi} \ln^2 \frac{\tau^{cut}}{Q} \right], \quad (\text{A.12})$$

the order α_s expansion of Eq. (3.2).

B Translation of two-loop corrections to the hard function

For the $W^\pm\gamma$, $Z\gamma$ and $\gamma\gamma$ processes presented in Refs. [90, 134] the finite remainders of the two-loop matrix elements remove singular terms of the form specified by Catani in Ref. [151] but without a factor of $(-\mu^2/s)^{2\epsilon}$ in the hard radiation factor $\mathcal{H}^{(2)}(\epsilon)$. The translation from this scheme to a standard $\overline{\text{MS}}$ subtraction of the singularities, to obtain the hard functions H_{ij} introduced in section 2, has been described in Ref. [152]. The implementation of this conversion has been discussed in some detail for these processes in Refs. [30, 31, 35].⁴

For the diboson (W^+W^- , $W^\pm Z$, ZZ) processes presented in Ref. [91] the finite remainders are presented in two schemes, in which the singularities are subtracted according either to exactly Catani's scheme [151] or to a scheme that is well-suited for the original formulation of q_T subtraction [153]. Starting from the latter ($\Omega_{q_T}^{(n),\text{finite}}$), we convert to amplitudes that enter the hard function ($\Omega_H^{(n),\text{finite}}$) using the relations,

$$\begin{aligned} \Omega_H^{(0),\text{finite}} &= \Omega_{q_T}^{(0),\text{finite}}, \\ \Omega_H^{(1),\text{finite}} &= \Omega_{q_T}^{(1),\text{finite}} + \Delta I_1 \Omega_{q_T}^{(0),\text{finite}}, \\ \Omega_H^{(2),\text{finite}} &= \Omega_{q_T}^{(2),\text{finite}} + \Delta I_1 \Omega_{q_T}^{(1),\text{finite}} + \Delta I_2 \Omega_{q_T}^{(0),\text{finite}}, \end{aligned} \quad (\text{B.1})$$

where the coefficients are given by,

$$\Delta I_1 = C_F \left[\frac{\pi^2}{12} - \left(\frac{3}{2} + i\pi \right) L - \frac{L^2}{2} \right], \quad (\text{B.2})$$

$$\begin{aligned} \Delta I_2 &= C_F^2 \left[\frac{\pi^4}{288} + \left(-\frac{3}{8} + \frac{3\pi^2}{8} - 6\zeta_3 - \frac{i\pi^3}{12} \right) L \right. \\ &\quad \left. + \left(\frac{9}{8} - \frac{13\pi^2}{24} + \frac{3i\pi}{2} \right) L^2 + \left(\frac{3}{4} + \frac{i\pi}{2} \right) L^3 + \frac{L^4}{8} \right] \end{aligned}$$

⁴arXiv:1603.02663v3 corrects typographical errors in previous versions of Ref. [35].

photon cuts	$p_{T,\gamma_1} > 40 \text{ GeV}, p_{T,\gamma_2} > 25 \text{ GeV}, \eta_\gamma < 2.5$
photon isolation	Frixione isolation with $n = 1, \varepsilon = 0.5$ and $\delta_0 = 0.4$
jet definition	anti- k_T algorithm with $R = 0.4$; $p_{T,j} > 25 \text{ GeV}, \eta_j < 4.5$

Table 7. Fiducial cuts for the $\gamma\gamma$ process.

	$pp \rightarrow e^- e^+ \gamma$	$pp \rightarrow e^- \bar{\nu}_e \gamma / pp \rightarrow e^+ \nu_e \gamma$
lepton cuts	$p_{T,\ell} > 25 \text{ GeV}, \eta_\ell < 2.47$ $m_{\ell-\ell^+} > 40 \text{ GeV}$	$p_{T,\ell} > 25 \text{ GeV}, \eta_\ell < 2.47$
photon cuts	$p_{T,\gamma} > 15 \text{ GeV}, \eta_\gamma < 2.37$	$p_{T,\gamma} > 15 \text{ GeV}, \eta_\gamma < 2.37$
neutrino cuts	n/a	$p_T^{\text{miss}} > 35 \text{ GeV}$
separation cuts:	$\Delta R_{\ell j} > 0.3, \Delta R_{\gamma j} > 0.3, \Delta R_{\ell\gamma} > 0.7$	
photon isolation	Frixione isolation with $n = 1, \varepsilon = 0.5$ and $\delta_0 = 0.4$	
jet definition	anti- k_T algorithm with $R = 0.4$; $p_{T,j} > 30 \text{ GeV}, \eta_j < 4.4$	

Table 8. Fiducial cuts for the $pp \rightarrow e^- e^+ \gamma$ ($Z\gamma$) and $pp \rightarrow e^- \bar{\nu}_e \gamma / pp \rightarrow e^+ \nu_e \gamma$ ($W^\pm \gamma$) processes.

$$\begin{aligned}
& +C_F C_A \left(-\frac{607}{162} + \frac{67\pi^2}{144} - \frac{\pi^4}{72} + \frac{77\zeta_3}{36} + \frac{11i\pi^3}{72} \right. \\
& \quad \left. - \left(\frac{961}{216} + \frac{11\pi^2}{36} - \frac{13\zeta_3}{2} + \frac{67i\pi}{18} - \frac{i\pi^3}{6} \right) L - \left(\frac{233}{72} + \frac{11i\pi}{12} - \frac{\pi^2}{12} \right) L^2 - \frac{11L^3}{36} \right] \\
& +C_F n_f (2T_R) \left[\frac{41}{81} - \frac{5\pi^2}{72} - \frac{7\zeta_3}{18} - \frac{i\pi^3}{36} + \left(\frac{65}{108} + \frac{\pi^2}{18} + \frac{5i\pi}{9} \right) L \right. \\
& \quad \left. + \left(\frac{19}{36} + \frac{i\pi}{6} \right) L^2 + \frac{L^3}{18} \right]. \tag{B.3}
\end{aligned}$$

In these formulae the logarithm is $L = \log(\mu^2/s_{12})$ and analytic continuation has already been performed assuming $s_{12} > 0$. As usual $C_F = 4/3$, $C_A = 3$ and $\zeta_3 = 1.20205690\dots$. Setting $L = 0$ reproduces the conversion factors presented in Eq. (2.9) of Ref. [1]. After conversion in this way the amplitudes are suitable for implementation in MCFM.

C Cuts

The fiducial cuts for the $\gamma\gamma$ production process are given in Table 7, for $Z\gamma$ and $W^\pm \gamma$ production processes in Table 8, for WW and $W^\pm Z$ production processes in Table 9, and for ZZ processes in Table 10. These cuts have been deliberately chosen to be the same as Ref. [24].

	$pp \rightarrow e^- \mu^+ \nu_\mu \bar{\nu}_e$	$pp \rightarrow e \nu_e \mu^+ \mu^-$
lepton cuts	$p_{T,\ell_1} > 25 \text{ GeV}, p_{T,\ell_2} > 20 \text{ GeV}$ $ \eta_e < 2.47, \eta_e \notin [1.37; 1.52]$ $ \eta_\mu < 2.4, m_{\ell-\ell^+} > 10 \text{ GeV}$	$p_{T,\mu} > 15 \text{ GeV}, p_{T,e} > 20 \text{ GeV}$ $ \eta_\ell < 2.5$ $ m_{\mu^+\mu^-} - m_Z < 10 \text{ GeV}$
neutrino cuts	$p_T^{\text{miss}} > 30 \text{ GeV}, p_T^{\text{miss,rel}} > 15 \text{ GeV}$	$m_{T,W} > 30 \text{ GeV}$
separation cuts	$\Delta R_{\ell\ell} > 0.1$	$\Delta R_{\mu\mu} > 0.2, \Delta R_{\mu e} > 0.3$
jet cuts	$N_{\text{jets}} = 0$	none
jet definition	anti- k_T algorithm with $R = 0.4$; $p_{T,j} > 25 \text{ GeV}, \eta_j < 4.5$	

Table 9. Fiducial cuts for the $pp \rightarrow e^- \mu^+ \nu_\mu \bar{\nu}_e$ (WW) and $pp \rightarrow e \nu_e \mu^+ \mu^-$ ($W^\pm Z$) processes.

lepton cuts	$p_{T,\ell} > 7 \text{ GeV}, \eta_\ell < 2.7, 66 \text{ GeV} < m_{\ell-\ell^+} < 116 \text{ GeV}$
separation cuts	$\Delta R_{\ell\ell} > 0.2$
jet definition	anti- k_T algorithm with $R = 0.4$; $p_{T,j} > 25 \text{ GeV}, \eta_j < 4.5$

Table 10. Fiducial cuts for the $pp \rightarrow e^- e^+ \mu^- \mu^+$ (ZZ) process.

References

- [1] G. Heinrich, S. Jahn, S.P. Jones, M. Kerner and J. Pires, *NNLO predictions for Z-boson pair production at the LHC*, *JHEP* **03** (2018) 142 [[1710.06294](#)].
- [2] M. Cepeda et al., *Report from Working Group 2: Higgs Physics at the HL-LHC and HE-LHC*, *CERN Yellow Rep. Monogr.* **7** (2019) 221 [[1902.00134](#)].
- [3] J.M. Campbell and R.K. Ellis, *An Update on vector boson pair production at hadron colliders*, *Phys. Rev. D* **60** (1999) 113006 [[hep-ph/9905386](#)].
- [4] J.M. Campbell, R.K. Ellis and C. Williams, *Vector boson pair production at the LHC*, *JHEP* **07** (2011) 018 [[1105.0020](#)].
- [5] J.M. Campbell, R.K. Ellis and W.T. Giele, *A Multi-Threaded Version of MCFM*, *Eur. Phys. J. C* **75** (2015) 246 [[1503.06182](#)].
- [6] J. Campbell and T. Neumann, *Precision Phenomenology with MCFM*, *JHEP* **12** (2019) 034 [[1909.09117](#)].
- [7] I.W. Stewart, F.J. Tackmann and W.J. Waalewijn, *N-Jettiness: An Inclusive Event Shape to Veto Jets*, *Phys. Rev. Lett.* **105** (2010) 092002 [[1004.2489](#)].
- [8] R. Boughezal, C. Focke, X. Liu and F. Petriello, *W-boson production in association with a jet at next-to-next-to-leading order in perturbative QCD*, *Phys. Rev. Lett.* **115** (2015) 062002 [[1504.02131](#)].

- [9] J. Gaunt, M. Stahlhofen, F.J. Tackmann and J.R. Walsh, *N-jettiness Subtractions for NNLO QCD Calculations*, *JHEP* **09** (2015) 058 [[1505.04794](#)].
- [10] S. Catani and M. Grazzini, *An NNLO subtraction formalism in hadron collisions and its application to Higgs boson production at the LHC*, *Phys. Rev. Lett.* **98** (2007) 222002 [[hep-ph/0703012](#)].
- [11] R. Boughezal, J.M. Campbell, R.K. Ellis, C. Focke, W.T. Giele, X. Liu et al., *Z-boson production in association with a jet at next-to-next-to-leading order in perturbative QCD*, *Phys. Rev. Lett.* **116** (2016) 152001 [[1512.01291](#)].
- [12] J.M. Campbell, R.K. Ellis and C. Williams, *Direct Photon Production at Next-to-Next-to-Leading Order*, *Phys. Rev. Lett.* **118** (2017) 222001 [[1612.04333](#)].
- [13] J.M. Campbell, R.K. Ellis and S. Seth, *H + 1 jet production revisited*, *JHEP* **10** (2019) 136 [[1906.01020](#)].
- [14] R. Mondini and C. Williams, *Bottom-induced contributions to Higgs plus jet at next-to-next-to-leading order*, *JHEP* **05** (2021) 045 [[2102.05487](#)].
- [15] G. Heinrich, *Collider Physics at the Precision Frontier*, *Phys. Rept.* **922** (2021) 1 [[2009.00516](#)].
- [16] C. Anastasiou, K. Melnikov and F. Petriello, *Higgs boson production at hadron colliders: Differential cross sections through next-to-next-to-leading order*, *Phys. Rev. Lett.* **93** (2004) 262002 [[hep-ph/0409088](#)].
- [17] C. Anastasiou, K. Melnikov and F. Petriello, *Fully differential Higgs boson production and the di-photon signal through next-to-next-to-leading order*, *Nucl. Phys. B* **724** (2005) 197 [[hep-ph/0501130](#)].
- [18] B. Mistlberger, *Higgs boson production at hadron colliders at N³LO in QCD*, *JHEP* **05** (2018) 028 [[1802.00833](#)].
- [19] L. Cieri, X. Chen, T. Gehrmann, E.W.N. Glover and A. Huss, *Higgs boson production at the LHC using the q_T subtraction formalism at N³LO QCD*, *JHEP* **02** (2019) 096 [[1807.11501](#)].
- [20] X. Chen, T. Gehrmann, E.W.N. Glover, A. Huss, B. Mistlberger and A. Pelloni, *Fully Differential Higgs Boson Production to Third Order in QCD*, *Phys. Rev. Lett.* **127** (2021) 072002 [[2102.07607](#)].
- [21] R. Boughezal, J.M. Campbell, R.K. Ellis, C. Focke, W. Giele, X. Liu et al., *Color singlet production at NNLO in MCFM*, *Eur. Phys. J. C* **77** (2017) 7 [[1605.08011](#)].
- [22] K. Melnikov and F. Petriello, *The W boson production cross section at the LHC through O(α_s^2)*, *Phys. Rev. Lett.* **96** (2006) 231803 [[hep-ph/0603182](#)].
- [23] S. Catani, L. Cieri, G. Ferrera, D. de Florian and M. Grazzini, *Vector boson production at hadron colliders: a fully exclusive QCD calculation at NNLO*, *Phys. Rev. Lett.* **103** (2009) 082001 [[0903.2120](#)].
- [24] M. Grazzini, S. Kallweit and M. Wiesemann, *Fully differential NNLO computations with MATRIX*, *Eur. Phys. J. C* **78** (2018) 537 [[1711.06631](#)].
- [25] K. Melnikov and F. Petriello, *Electroweak gauge boson production at hadron colliders through O(α_s^2)*, *Phys. Rev. D* **74** (2006) 114017 [[hep-ph/0609070](#)].
- [26] G. Ferrera, M. Grazzini and F. Tramontano, *Associated ZH production at hadron colliders: the fully differential NNLO QCD calculation*, *Phys. Lett. B* **740** (2015) 51 [[1407.4747](#)].
- [27] J.M. Campbell, R.K. Ellis and C. Williams, *Associated production of a Higgs boson at NNLO*, *JHEP* **06** (2016) 179 [[1601.00658](#)].

- [28] M. Grazzini, S. Kallweit and D. Rathlev, $W\gamma$ and $Z\gamma$ production at the LHC in NNLO QCD, *JHEP* **07** (2015) 085 [[1504.01330](#)].
- [29] T. Cridge, M.A. Lim and R. Nagar, $W\gamma$ production at NNLO+PS accuracy in GENEVA, [2105.13214](#).
- [30] J.M. Campbell, G. De Laurentis, R.K. Ellis and S. Seth, $pp \rightarrow W(\rightarrow l\nu) + \gamma$ process at next-to-next-to-leading order, [2105.00954](#).
- [31] J.M. Campbell, T. Neumann and C. Williams, $Z\gamma$ Production at NNLO Including Anomalous Couplings, *JHEP* **11** (2017) 150 [[1708.02925](#)].
- [32] S. Catani, L. Cieri, D. de Florian, G. Ferrera and M. Grazzini, Diphoton production at hadron colliders: a fully-differential QCD calculation at NNLO, *Phys. Rev. Lett.* **108** (2012) 072001 [[1110.2375](#)].
- [33] S. Catani, L. Cieri, D. de Florian, G. Ferrera and M. Grazzini, Diphoton production at the LHC: a QCD study up to NNLO, *JHEP* **04** (2018) 142 [[1802.02095](#)].
- [34] S. Alioli, A. Broggio, A. Gavardi, S. Kallweit, M.A. Lim, R. Nagar et al., Precise predictions for photon pair production matched to parton showers in GENEVA, *JHEP* **04** (2021) 041 [[2010.10498](#)].
- [35] J.M. Campbell, R.K. Ellis, Y. Li and C. Williams, Predictions for diphoton production at the LHC through NNLO in QCD, *JHEP* **07** (2016) 148 [[1603.02663](#)].
- [36] M. Brucherseifer, F. Caola and K. Melnikov, On the NNLO QCD corrections to single-top production at the LHC, *Phys. Lett. B* **736** (2014) 58 [[1404.7116](#)].
- [37] J. Campbell, T. Neumann and Z. Sullivan, Single-top-quark production in the t -channel at NNLO, *JHEP* **02** (2021) 040 [[2012.01574](#)].
- [38] G. Ferrera, M. Grazzini and F. Tramontano, Higher-order QCD effects for associated WH production and decay at the LHC, *JHEP* **04** (2014) 039 [[1312.1669](#)].
- [39] F. Caola, G. Luisoni, K. Melnikov and R. Rötsch, NNLO QCD corrections to associated WH production and $H \rightarrow b\bar{b}$ decay, *Phys. Rev. D* **97** (2018) 074022 [[1712.06954](#)].
- [40] M. Grazzini, S. Kallweit, D. Rathlev and M. Wiesemann, $W^\pm Z$ production at hadron colliders in NNLO QCD, *Phys. Lett. B* **761** (2016) 179 [[1604.08576](#)].
- [41] M. Grazzini, S. Kallweit, D. Rathlev and M. Wiesemann, $W^\pm Z$ production at the LHC: fiducial cross sections and distributions in NNLO QCD, *JHEP* **05** (2017) 139 [[1703.09065](#)].
- [42] F. Cascioli, T. Gehrmann, M. Grazzini, S. Kallweit, P. Maierhöfer, A. von Manteuffel et al., ZZ production at hadron colliders in NNLO QCD, *Phys. Lett. B* **735** (2014) 311 [[1405.2219](#)].
- [43] M. Grazzini, S. Kallweit and D. Rathlev, ZZ production at the LHC: fiducial cross sections and distributions in NNLO QCD, *Phys. Lett. B* **750** (2015) 407 [[1507.06257](#)].
- [44] F. Caola, K. Melnikov, R. Rötsch and L. Tancredi, QCD corrections to ZZ production in gluon fusion at the LHC, *Phys. Rev. D* **92** (2015) 094028 [[1509.06734](#)].
- [45] S. Kallweit and M. Wiesemann, ZZ production at the LHC: NNLO predictions for $2\ell 2\nu$ and 4ℓ signatures, *Phys. Lett. B* **786** (2018) 382 [[1806.05941](#)].
- [46] M. Grazzini, S. Kallweit, M. Wiesemann and J.Y. Yook, ZZ production at the LHC: NLO QCD corrections to the loop-induced gluon fusion channel, *JHEP* **03** (2019) 070 [[1811.09593](#)].
- [47] T. Gehrmann, M. Grazzini, S. Kallweit, P. Maierhöfer, A. von Manteuffel, S. Pozzorini et al., W^+W^- Production at Hadron Colliders in Next to Next to Leading Order QCD, *Phys. Rev. Lett.* **113** (2014) 212001 [[1408.5243](#)].

- [48] F. Caola, K. Melnikov, R. Röntsch and L. Tancredi, *QCD corrections to W^+W^- production through gluon fusion*, *Phys. Lett. B* **754** (2016) 275 [[1511.08617](#)].
- [49] M. Grazzini, S. Kallweit, S. Pozzorini, D. Rathlev and M. Wiesemann, *W^+W^- production at the LHC: fiducial cross sections and distributions in NNLO QCD*, *JHEP* **08** (2016) 140 [[1605.02716](#)].
- [50] M. Grazzini, S. Kallweit, M. Wiesemann and J.Y. Yook, *W^+W^- production at the LHC: NLO QCD corrections to the loop-induced gluon fusion channel*, *Phys. Lett. B* **804** (2020) 135399 [[2002.01877](#)].
- [51] R. Boughezal, X. Liu and F. Petriello, *W-boson plus jet differential distributions at NNLO in QCD*, *Phys. Rev. D* **94** (2016) 113009 [[1602.06965](#)].
- [52] A. Gehrmann-De Ridder, T. Gehrmann, E.W.N. Glover, A. Huss and D.M. Walker, *Next-to-Next-to-Leading-Order QCD Corrections to the Transverse Momentum Distribution of Weak Gauge Bosons*, *Phys. Rev. Lett.* **120** (2018) 122001 [[1712.07543](#)].
- [53] A. Gehrmann-De Ridder, T. Gehrmann, E.W.N. Glover, A. Huss and T.A. Morgan, *Precise QCD predictions for the production of a Z boson in association with a hadronic jet*, *Phys. Rev. Lett.* **117** (2016) 022001 [[1507.02850](#)].
- [54] A. Gehrmann-De Ridder, T. Gehrmann, E.W.N. Glover, A. Huss and T.A. Morgan, *The NNLO QCD corrections to Z boson production at large transverse momentum*, *JHEP* **07** (2016) 133 [[1605.04295](#)].
- [55] X. Chen, T. Gehrmann, N. Glover, M. Höfer and A. Huss, *Isolated photon and photon+jet production at NNLO QCD accuracy*, *JHEP* **04** (2020) 166 [[1904.01044](#)].
- [56] R. Boughezal, F. Caola, K. Melnikov, F. Petriello and M. Schulze, *Higgs boson production in association with a jet at next-to-next-to-leading order in perturbative QCD*, *JHEP* **06** (2013) 072 [[1302.6216](#)].
- [57] X. Chen, T. Gehrmann, E.W.N. Glover and M. Jaquier, *Precise QCD predictions for the production of Higgs + jet final states*, *Phys. Lett. B* **740** (2015) 147 [[1408.5325](#)].
- [58] R. Boughezal, F. Caola, K. Melnikov, F. Petriello and M. Schulze, *Higgs boson production in association with a jet at next-to-next-to-leading order*, *Phys. Rev. Lett.* **115** (2015) 082003 [[1504.07922](#)].
- [59] R. Boughezal, C. Focke, W. Giele, X. Liu and F. Petriello, *Higgs boson production in association with a jet at NNLO using jetiness subtraction*, *Phys. Lett. B* **748** (2015) 5 [[1505.03893](#)].
- [60] F. Caola, K. Melnikov and M. Schulze, *Fiducial cross sections for Higgs boson production in association with a jet at next-to-next-to-leading order in QCD*, *Phys. Rev. D* **92** (2015) 074032 [[1508.02684](#)].
- [61] X. Chen, T. Gehrmann, N. Glover and M. Jaquier, *Higgs plus one jet production at NNLO*, *PoS RADCOR2015* (2016) 056 [[1604.04085](#)].
- [62] M. Czakon, P. Fiedler, D. Heymes and A. Mitov, *NNLO QCD predictions for fully-differential top-quark pair production at the Tevatron*, *JHEP* **05** (2016) 034 [[1601.05375](#)].
- [63] G. Abelof, A. Gehrmann-De Ridder and I. Majer, *Top quark pair production at NNLO in the quark-antiquark channel*, *JHEP* **12** (2015) 074 [[1506.04037](#)].
- [64] S. Catani, S. Devoto, M. Grazzini, S. Kallweit and J. Mazzitelli, *Top-quark pair production at the LHC: Fully differential QCD predictions at NNLO*, *JHEP* **07** (2019) 100 [[1906.06535](#)].

- [65] S. Catani, S. Devoto, M. Grazzini, S. Kallweit, J. Mazzitelli and H. Sargsyan, *Top-quark pair hadroproduction at next-to-next-to-leading order in QCD*, *Phys. Rev. D* **99** (2019) 051501 [[1901.04005](#)].
- [66] M. Czakon, A. Mitov and R. Poncelet, *NNLO QCD corrections to leptonic observables in top-quark pair production and decay*, *JHEP* **05** (2021) 212 [[2008.11133](#)].
- [67] S. Catani, S. Devoto, M. Grazzini, S. Kallweit and J. Mazzitelli, *Top-quark pair hadroproduction at NNLO: differential predictions with the \overline{MS} mass*, *JHEP* **08** (2020) 027 [[2005.00557](#)].
- [68] R. Gauld, A. Gehrmann-De Ridder, E.W.N. Glover, A. Huss and I. Majer, *Predictions for Z -Boson Production in Association with a b-Jet at $\mathcal{O}(\alpha_s^3)$* , *Phys. Rev. Lett.* **125** (2020) 222002 [[2005.03016](#)].
- [69] R. Gauld, A. Gehrmann-De Ridder, E.W.N. Glover, A. Huss and I. Majer, *Precise predictions for WH+jet production at the LHC*, *Phys. Lett. B* **817** (2021) 136335 [[2009.14209](#)].
- [70] R. Gauld, A. Gehrmann-De Ridder, E.W.N. Glover, A. Huss and I. Majer, *VH + jet production in hadron-hadron collisions up to order α_s^3 in perturbative QCD*, [2110.12992](#).
- [71] M. Cacciari, F.A. Dreyer, A. Karlberg, G.P. Salam and G. Zanderighi, *Fully Differential Vector-Boson-Fusion Higgs Production at Next-to-Next-to-Leading Order*, *Phys. Rev. Lett.* **115** (2015) 082002 [[1506.02660](#)].
- [72] A. Buckley et al., *A comparative study of Higgs boson production from vector-boson fusion*, [2105.11399](#).
- [73] C. Anastasiou, F. Herzog and A. Lazopoulos, *The fully differential decay rate of a Higgs boson to bottom-quarks at NNLO in QCD*, *JHEP* **03** (2012) 035 [[1110.2368](#)].
- [74] V. Del Duca, C. Duhr, G. Somogyi, F. Tramontano and Z. Trócsányi, *Higgs boson decay into b-quarks at NNLO accuracy*, *JHEP* **04** (2015) 036 [[1501.07226](#)].
- [75] R. Mondini, M. Schiavi and C. Williams, *N^3LO predictions for the decay of the Higgs boson to bottom quarks*, *JHEP* **06** (2019) 079 [[1904.08960](#)].
- [76] J. Gao, C.S. Li and H.X. Zhu, *Top Quark Decay at Next-to-Next-to Leading Order in QCD*, *Phys. Rev. Lett.* **110** (2013) 042001 [[1210.2808](#)].
- [77] M. Brucherseifer, F. Caola and K. Melnikov, *$\mathcal{O}(\alpha_s^2)$ corrections to fully-differential top quark decays*, *JHEP* **04** (2013) 059 [[1301.7133](#)].
- [78] J. Currie, A. Gehrmann-De Ridder, T. Gehrmann, N. Glover, J. Pires and S. Wells, *Second order QCD corrections to gluonic jet production at hadron colliders*, *PoS LL2014* (2014) 001 [[1407.5558](#)].
- [79] J. Currie, E.W.N. Glover and J. Pires, *Next-to-Next-to Leading Order QCD Predictions for Single Jet Inclusive Production at the LHC*, *Phys. Rev. Lett.* **118** (2017) 072002 [[1611.01460](#)].
- [80] A. Gehrmann-De Ridder, T. Gehrmann, E.W.N. Glover, A. Huss and J. Pires, *Triple Differential Dijet Cross Section at the LHC*, *Phys. Rev. Lett.* **123** (2019) 102001 [[1905.09047](#)].
- [81] H.A. Chawdhry, M. Czakon, A. Mitov and R. Poncelet, *NNLO QCD corrections to diphoton production with an additional jet at the LHC*, [2105.06940](#).
- [82] M. Czakon, A. Mitov, M. Pellen and R. Poncelet, *NNLO QCD predictions for W+c-jet production at the LHC*, [2011.01011](#).

- [83] S. Catani, S. Devoto, M. Grazzini, S. Kallweit and J. Mazzitelli, *Bottom-quark production at hadron colliders: fully differential predictions in NNLO QCD*, *JHEP* **03** (2021) 029 [[2010.11906](#)].
- [84] H.A. Chawdhry, M.L. Czakon, A. Mitov and R. Poncelet, *NNLO QCD corrections to three-photon production at the LHC*, *JHEP* **02** (2020) 057 [[1911.00479](#)].
- [85] S. Kallweit, V. Sotnikov and M. Wiesemann, *Triphoton production at hadron colliders in NNLO QCD*, *Phys. Lett. B* **812** (2021) 136013 [[2010.04681](#)].
- [86] M. Grazzini, G. Heinrich, S. Jones, S. Kallweit, M. Kerner, J.M. Lindert et al., *Higgs boson pair production at NNLO with top quark mass effects*, *JHEP* **05** (2018) 059 [[1803.02463](#)].
- [87] D. de Florian, I. Fabre and J. Mazzitelli, *Triple Higgs production at hadron colliders at NNLO in QCD*, *JHEP* **03** (2020) 155 [[1912.02760](#)].
- [88] M. Grazzini, S. Kallweit, J.M. Lindert, S. Pozzorini and M. Wiesemann, *NNLO QCD + NLO EW with Matrix+OpenLoops: precise predictions for vector-boson pair production*, *JHEP* **02** (2020) 087 [[1912.00068](#)].
- [89] F. Buccioni, J.-N. Lang, J.M. Lindert, P. Maierhöfer, S. Pozzorini, H. Zhang et al., *OpenLoops 2*, *Eur. Phys. J. C* **79** (2019) 866 [[1907.13071](#)].
- [90] T. Gehrmann and L. Tancredi, *Two-loop QCD helicity amplitudes for $q\bar{q} \rightarrow W^\pm \gamma$ and $q\bar{q} \rightarrow Z^0 \gamma$* , *JHEP* **02** (2012) 004 [[1112.1531](#)].
- [91] T. Gehrmann, A. von Manteuffel and L. Tancredi, *The two-loop helicity amplitudes for $q\bar{q}' \rightarrow V_1 V_2 \rightarrow 4$ leptons*, *JHEP* **09** (2015) 128 [[1503.04812](#)].
- [92] S. Alekhin, A. Kardos, S. Moch and Z. Trócsányi, *Precision studies for Drell-Yan processes at NNLO*, [2104.02400](#).
- [93] G.P. Salam and E. Slade, *Cuts for two-body decays at colliders*, *JHEP* **11** (2021) 220 [[2106.08329](#)].
- [94] L. Buonocore, S. Kallweit, L. Rottoli and M. Wiesemann, *Linear power corrections for two-body kinematics in the q_T subtraction formalism*, [2111.13661](#).
- [95] S. Camarda, L. Cieri and G. Ferrera, *Fiducial perturbative power corrections within the q_T subtraction formalism*, [2111.14509](#).
- [96] T. Becher and T. Neumann, *Fiducial q_T resummation of color-singlet processes at $N^3LL+NNLO$* , *JHEP* **03** (2021) 199 [[2009.11437](#)].
- [97] T. Neumann, *The diphoton q_T spectrum at $N^3LL' + NNLO$* , *Eur. Phys. J. C* **81** (2021) 905 [[2107.12478](#)].
- [98] M. Grazzini, S. Kallweit, D. Rathlev and M. Wiesemann, *Transverse-momentum resummation for vector-boson pair production at NNLL+NNLO*, *JHEP* **08** (2015) 154 [[1507.02565](#)].
- [99] S. Kallweit, E. Re, L. Rottoli and M. Wiesemann, *Accurate single- and double-differential resummation of colour-singlet processes with MATRIX+RADISH: W^+W^- production at the LHC*, *JHEP* **12** (2020) 147 [[2004.07720](#)].
- [100] M. Wiesemann, L. Rottoli and P. Torrielli, *The $Z\gamma$ transverse-momentum spectrum at NNLO+N³LL*, *Phys. Lett. B* **809** (2020) 135718 [[2006.09338](#)].
- [101] S. Alioli, A. Broggio and M.A. Lim, *Zero-jettiness resummation for top-quark pair production at the LHC*, *JHEP* **01** (2022) 066 [[2111.03632](#)].
- [102] C.W. Bauer, S. Fleming and M.E. Luke, *Summing Sudakov logarithms in $B \rightarrow X(s\gamma)$ in effective field theory*, *Phys. Rev. D* **63** (2000) 014006 [[hep-ph/0005275](#)].

- [103] C.W. Bauer, S. Fleming, D. Pirjol and I.W. Stewart, *An Effective field theory for collinear and soft gluons: Heavy to light decays*, *Phys. Rev. D* **63** (2001) 114020 [[hep-ph/0011336](#)].
- [104] C.W. Bauer and I.W. Stewart, *Invariant operators in collinear effective theory*, *Phys. Lett. B* **516** (2001) 134 [[hep-ph/0107001](#)].
- [105] C.W. Bauer, D. Pirjol and I.W. Stewart, *Soft collinear factorization in effective field theory*, *Phys. Rev. D* **65** (2002) 054022 [[hep-ph/0109045](#)].
- [106] C.W. Bauer, S. Fleming, D. Pirjol, I.Z. Rothstein and I.W. Stewart, *Hard scattering factorization from effective field theory*, *Phys. Rev. D* **66** (2002) 014017 [[hep-ph/0202088](#)].
- [107] J.R. Gaunt, M. Stahlhofen and F.J. Tackmann, *The Quark Beam Function at Two Loops*, *JHEP* **04** (2014) 113 [[1401.5478](#)].
- [108] J. Gaunt, M. Stahlhofen and F.J. Tackmann, *The Gluon Beam Function at Two Loops*, *JHEP* **08** (2014) 020 [[1405.1044](#)].
- [109] R. Kelley, M.D. Schwartz, R.M. Schabinger and H.X. Zhu, *The two-loop hemisphere soft function*, *Phys. Rev. D* **84** (2011) 045022 [[1105.3676](#)].
- [110] P.F. Monni, T. Gehrmann and G. Luisoni, *Two-Loop Soft Corrections and Resummation of the Thrust Distribution in the Dijet Region*, *JHEP* **08** (2011) 010 [[1105.4560](#)].
- [111] I. Moulton, L. Rothen, I.W. Stewart, F.J. Tackmann and H.X. Zhu, *Subleading Power Corrections for N -Jettiness Subtractions*, *Phys. Rev. D* **95** (2017) 074023 [[1612.00450](#)].
- [112] R. Boughezal, X. Liu and F. Petriello, *Power Corrections in the N -jettiness Subtraction Scheme*, *JHEP* **03** (2017) 160 [[1612.02911](#)].
- [113] R. Boughezal, A. Isgrò and F. Petriello, *Next-to-leading-logarithmic power corrections for N -jettiness subtraction in color-singlet production*, *Phys. Rev. D* **97** (2018) 076006 [[1802.00456](#)].
- [114] I. Moulton, L. Rothen, I.W. Stewart, F.J. Tackmann and H.X. Zhu, *N -jettiness subtractions for $gg \rightarrow H$ at subleading power*, *Phys. Rev. D* **97** (2018) 014013 [[1710.03227](#)].
- [115] M.A. Ebert, I. Moulton, I.W. Stewart, F.J. Tackmann, G. Vita and H.X. Zhu, *Power Corrections for N -Jettiness Subtractions at $\mathcal{O}(\alpha_s)$* , *JHEP* **12** (2018) 084 [[1807.10764](#)].
- [116] J.C. Collins and D.E. Soper, *Back-To-Back Jets in QCD*, *Nucl. Phys. B* **193** (1981) 381.
- [117] J.C. Collins, D.E. Soper and G.F. Sterman, *Transverse Momentum Distribution in Drell-Yan Pair and W and Z Boson Production*, *Nucl. Phys. B* **250** (1985) 199.
- [118] S. Catani, D. de Florian and M. Grazzini, *Universality of nonleading logarithmic contributions in transverse momentum distributions*, *Nucl. Phys. B* **596** (2001) 299 [[hep-ph/0008184](#)].
- [119] X.-d. Ji, J.-p. Ma and F. Yuan, *QCD factorization for semi-inclusive deep-inelastic scattering at low transverse momentum*, *Phys. Rev. D* **71** (2005) 034005 [[hep-ph/0404183](#)].
- [120] X.-d. Ji, J.-P. Ma and F. Yuan, *QCD factorization for spin-dependent cross sections in DIS and Drell-Yan processes at low transverse momentum*, *Phys. Lett. B* **597** (2004) 299 [[hep-ph/0405085](#)].
- [121] G. Bozzi, S. Catani, D. de Florian and M. Grazzini, *Transverse-momentum resummation and the spectrum of the Higgs boson at the LHC*, *Nucl. Phys. B* **737** (2006) 73 [[hep-ph/0508068](#)].
- [122] T. Becher and M. Neubert, *Drell-Yan Production at Small q_T , Transverse Parton Distributions and the Collinear Anomaly*, *Eur. Phys. J. C* **71** (2011) 1665 [[1007.4005](#)].
- [123] T. Becher, M. Neubert and D. Wilhelm, *Higgs-Boson Production at Small Transverse Momentum*, *JHEP* **05** (2013) 110 [[1212.2621](#)].

- [124] T. Gehrmann, T. Luebbert and L.L. Yang, *Calculation of the transverse parton distribution functions at next-to-next-to-leading order*, *JHEP* **06** (2014) 155 [[1403.6451](#)].
- [125] G. Billis, M.A. Ebert, J.K.L. Michel and F.J. Tackmann, *A toolbox for q_T and 0-jettiness subtractions at N^3LO* , *Eur. Phys. J. Plus* **136** (2021) 214 [[1909.00811](#)].
- [126] M.A. Ebert, I. Moulton, I.W. Stewart, F.J. Tackmann, G. Vita and H.X. Zhu, *Subleading power rapidity divergences and power corrections for q_T* , *JHEP* **04** (2019) 123 [[1812.08189](#)].
- [127] L. Cieri, C. Oleari and M. Rocco, *Higher-order power corrections in a transverse-momentum cut for colour-singlet production at NLO*, *Eur. Phys. J. C* **79** (2019) 852 [[1906.09044](#)].
- [128] C. Oleari and M. Rocco, *Power corrections in a transverse-momentum cut for vector-boson production at NNLO: the qg -initiated real-virtual contribution*, *Eur. Phys. J. C* **81** (2021) 183 [[2012.10538](#)].
- [129] T. Matsuura and W.L. van Neerven, *Second Order Logarithmic Corrections to the Drell-Yan Cross-section*, *Z. Phys. C* **38** (1988) 623.
- [130] T. Gehrmann, T. Huber and D. Maitre, *Two-loop quark and gluon form-factors in dimensional regularisation*, *Phys. Lett. B* **622** (2005) 295 [[hep-ph/0507061](#)].
- [131] S. Dawson, *Radiative corrections to Higgs boson production*, *Nucl. Phys. B* **359** (1991) 283.
- [132] A. Djouadi, M. Spira and P.M. Zerwas, *Production of Higgs bosons in proton colliders: QCD corrections*, *Phys. Lett. B* **264** (1991) 440.
- [133] V. Ahrens, T. Becher, M. Neubert and L.L. Yang, *Renormalization-Group Improved Prediction for Higgs Production at Hadron Colliders*, *Eur. Phys. J. C* **62** (2009) 333 [[0809.4283](#)].
- [134] C. Anastasiou, E.W.N. Glover and M.E. Tejeda-Yeomans, *Two loop QED and QCD corrections to massless fermion boson scattering*, *Nucl. Phys. B* **629** (2002) 255 [[hep-ph/0201274](#)].
- [135] L. Naterop, A. Signer and Y. Ulrich, *handyG —Rapid numerical evaluation of generalised polylogarithms in Fortran*, *Comput. Phys. Commun.* **253** (2020) 107165 [[1909.01656](#)].
- [136] J.M. Campbell, D.J. Miller and T. Robens, *Next-to-Leading Order Predictions for $WW+Jet$ Production*, *Phys. Rev. D* **92** (2015) 014033 [[1506.04801](#)].
- [137] J.M. Campbell, G. De Laurentis and R.K. Ellis, *Vector boson pair production at one loop: analytic results for the process $q\bar{q}\ell\ell'g$* , [2203.17170](#).
- [138] S. Actis, A. Denner, L. Hofer, J.-N. Lang, A. Scharf and S. Uccirati, *RECOLA: REcursive Computation of One-Loop Amplitudes*, *Comput. Phys. Commun.* **214** (2017) 140 [[1605.01090](#)].
- [139] A. Denner, J.-N. Lang and S. Uccirati, *Recola2: REcursive Computation of One-Loop Amplitudes 2*, *Comput. Phys. Commun.* **224** (2018) 346 [[1711.07388](#)].
- [140] J.M. Campbell, S. Höche and C.T. Preuss, *Accelerating LHC phenomenology with analytic one-loop amplitudes: A C++ interface to MCFM*, *Eur. Phys. J. C* **81** (2021) 1117 [[2107.04472](#)].
- [141] C.F. Berger, C. Marcantonini, I.W. Stewart, F.J. Tackmann and W.J. Waalewijn, *Higgs Production with a Central Jet Veto at NNLL+NNLO*, *JHEP* **04** (2011) 092 [[1012.4480](#)].
- [142] A. Denner and S. Dittmaier, *The Complex-mass scheme for perturbative calculations with unstable particles*, *Nucl. Phys. B Proc. Suppl.* **160** (2006) 22 [[hep-ph/0605312](#)].
- [143] PARTICLE DATA GROUP collaboration, *Review of Particle Physics*, *Chin. Phys. C* **40** (2016) 100001.

- [144] NNPDF collaboration, *Parton distributions for the LHC Run II*, *JHEP* **04** (2015) 040 [[1410.8849](#)].
- [145] R.K. Ellis, D.A. Ross and A.E. Terrano, *The Perturbative Calculation of Jet Structure in $e^+ e^-$ Annihilation*, *Nucl. Phys. B* **178** (1981) 421.
- [146] S. Catani and M.H. Seymour, *A General algorithm for calculating jet cross-sections in NLO QCD*, *Nucl. Phys. B* **485** (1997) 291 [[hep-ph/9605323](#)].
- [147] O. Brein, A. Djouadi and R. Harlander, *NNLO QCD corrections to the Higgs-strahlung processes at hadron colliders*, *Phys. Lett. B* **579** (2004) 149 [[hep-ph/0307206](#)].
- [148] O. Brein, R.V. Harlander and T.J.E. Zirke, *vh@nnlo - Higgs Strahlung at hadron colliders*, *Comput. Phys. Commun.* **184** (2013) 998 [[1210.5347](#)].
- [149] L. Buonocore, M. Grazzini, J. Haag, L. Rottoli and C. Savoini, *Effective transverse momentum in multiple jet production at hadron colliders*, [2201.11519](#).
- [150] S.D. Ellis and W.J. Stirling, *Quark Form-factors and Leading Double Logarithms in QCD*, *Phys. Rev. D* **23** (1981) 214.
- [151] S. Catani, *The Singular behavior of QCD amplitudes at two loop order*, *Phys. Lett. B* **427** (1998) 161 [[hep-ph/9802439](#)].
- [152] T. Becher, G. Bell, C. Lorentzen and S. Marti, *Transverse-momentum spectra of electroweak bosons near threshold at NNLO*, *JHEP* **02** (2014) 004 [[1309.3245](#)].
- [153] S. Catani, L. Cieri, D. de Florian, G. Ferrera and M. Grazzini, *Universality of transverse-momentum resummation and hard factors at the NNLO*, *Nucl. Phys. B* **881** (2014) 414 [[1311.1654](#)].